Quantum Chaos: from Minimal Models to Universality

Zusammenfassung ausgewählter Veröffentlichungen

zum Zwecke der Habilitation vorgelegt

an der Fakultät für Physik

der Georg-August-Universität Göttingen

von

Dr. Holger Schanz

aus Rudolstadt in Thüringen

Januar 2004

Abstract

In this manuscript a number of selected publications concerning the properties of quantum systems with a chaotic classical analogue are reviewed. Emphasis is placed on the description of spectrum and eigenstates in the semiclassical regime and also on transport properties in extended quasi one-dimensional systems.

Most of the presented results are obtained with the help of minimal models highlighting by construction certain universal aspects of quantum chaos. These models include billiards, Hamiltonian maps and quantum graphs, and they will be briefly introduced in the beginning.

The second part deals with the semiclassical theory of quantum two-point correlation functions such as the spectral form factor. The main topic is here the diagonal approximation and methods to improve it by accounting for action correlations between classical trajectories.

In the third and fourth chapters the localization of quantum eigenfunctions in classical phase space plays an important role. We discuss the effect of scarring on classical periodic orbits and stress in particular the difference between strong scarring in individual eigenstates and an enhanced average localization on the orbit which is, however, distributed over many states. We also discuss limitations to the applicability of the semiclassical eigenfunction hypothesis, which predicts that eigenstates are localized on a single invariant manifold of the classical phase space.

Finally transport properties in extended, periodic systems are addressed. These include the quantum manifestations of classical diffusion in the statistics of band spectra and the classical and quantum theory of Hamiltonian ratchets, that is systems in which directed ballistic transport occurs due to the simultaneous presence of regular and chaotic dynamics.

Contents

Chapter 1

Introduction

1.1 Background and scope

This manuscript contains an introduction to some selected publications of the author, highlighting their common theme and their interrelations more than a single paper typically does. We will explore quantum systems with a chaotic classical limit and address (i) the semiclassical description of correlations in spectral and dynamical quantities, (ii) the localization of quantum eigenstates in classical phase space and (iii) transport in quasi one-dimensional periodic systems and in particular in classical and quantum Hamiltonian ratchets.

Although these problems are quite diverse, they are all subsumed in the field of *quantum chaos* [1]–[9]. Its scope can be defined by quoting Michael Berry [10]: "Quantum chaology is the study of semiclassical, but nonclassical, phenomena characteristic of systems whose classical counterparts exhibit chaos.". Curiously the article containing this quotation was called "Quantum chaology, Not Quantum Chaos", but nevertheless the latter term remained a popular synonym for the former. No confusion should occur since chaos in its literal sense of exponential sensitivity to initial conditions is excluded in quantum mechanics due to the unitary and linear dynamics and the uncertainty principle.

One might add to the above definition that the phenomena collected and explained in quantum chaos are *universal*, i.e., independent of the concrete physical system as long as it has chaotic dynamics. As examples have served systems as diverse as nuclei [11]–[16], atoms [17]–[24] including Bose-Einstein

condensates [25], molecules [26], mesoscopic electronic structures [27]–[32], classical waves in macroscopic confinements (microwave billiards [33]–[39], microlasers [40]–[42], sound waves [43]–[47]) and even the dynamics of stars [48] or the universe [49] on cosmological scales. Clearly, the energy and time scales relevant for these systems could not be more different. However, according to a hypothesis put forward by Bohigas, Giannoni and Schmit [50], the *local* properties of the spectra, on the scale of one or a few mean level spacings, are universal in the presence of chaos.

What is more, these properties turned out to be the same for chaotic systems and suitable ensembles of random matrices. Random matrices had been introduced and studied before by Wigner, Dyson and others in order to describe the complicated and in detail unknown Hamiltonians of heavy nuclei [51, 52]. The application of random-matrix theory (RMT) to quantum chaos proved to be extremely successful. In particular there are very powerful analytical tools that allow to calculate virtually any quantity of interest within RMT [53]–[58]. The predictions obtained in this way do concern not only spectral statistics but also eigenstates, quantum dynamics, scattering amplitudes etc. and they did compare favourably with numerical and experimental data in numerous studies of chaotic systems.

Nevertheless there are important aspects of quantum chaos which cannot be accounted for by RMT alone because the latter discards any system-specific information other than basic symmetries. Such information about the individual chaotic system is retained in the semiclassical quantization by Gutzwiller's trace formula [59, 60] and encoded in the classical periodic orbits (PO's). As a consequence, these orbits are directly related to many universal phenomena beyond RMT. For example, the orbit with the shortest period shows up in the quantum spectral statistics as the maximal energy scale on which RMT does apply [61]. And *scarred* eigenstates, differing from the RMT prediction by an enhanced localization, are concentrated in phase space around some of the short PO's (see Chapter 3). So while the set of PO's is different for each particular system, the way they show up in the quantized version is the same. In this sense one can say that both, faithfulness to RMT predictions and traces left by the individual classical PO's are universal aspects of quantum chaos. However, the interrelation between these two approaches is not yet completely understood. In particular, the question how random-matrix behaviour emerges from periodic-orbit theory has recently attracted a lot of attention. Chapter 2 of this work will be related to this problem. It will become clear that periodic-orbit theory is applicable also in

situations where RMT fails due to specific features of the classical dynamics. An important example of this type is given by chaotic systems which are spatially periodic. We will discuss this case in Section 4.1.

Completely chaotic classical systems are as exceptional as completely integrable ones. Most systems have a mixed phase space with chaotic and regular dynamics being present simultaneously. In this generic case even the classical dynamics is far from being well understood. The main problem are the complex self-similar structures which exist in the phase space of a mixed system. Typically, an infinite number of smaller and smaller regular components are embedded in a chaotic background, which by itself is not homogeneous but contains hierarchies of cantori acting as partial transport barriers. While the description of these complicated substructures of a mixed phase space remains a largely unsolved problem, there exist also more tangible effects that are due to the coexistence of regular and chaotic dynamics. An interesting and important example is directed chaotic transport in extended systems with a periodic mixed phase space. We shall elucidate this novel phenomenon in Section 4.2.

As a first step towards understanding quantum systems with a mixed classical limit one may ignore the intricate phase-space structures at the border between regular and chaotic dynamics and make use of the *semiclassical eigenfunction hypothesis* which is due to Percival [62] and Berry [63]. According to this hypothesis, almost all eigenstates live in the semiclassical limit on a single invariant set of phase space, e.g., the chaotic sea or a regular island. Regular and chaotic components of phase space are then effectively decoupled and can be treated separately. For example, the spectral statistics is a superposition of the Poissonian distribution which is characteristic for integrability and the random-matrix prediction for chaos, weighted with the corresponding phase-space fractions [64]. Although recent results pointed out deviations from this simple picture at finite $\hbar$ [65]–[67], the semiclassical eigenfunction hypothesis remains the basic tool for understanding the behaviour of generic systems in the semiclassical regime. For example, application of it to Hamiltonian ratchets leads in a straightforward way to a theory of directed quantum transport, which is outlined in Section 4.3. In this Section we investigate also the eigenstates of extended mixed systems showing directed transport *in the absence* of exact quantum periodicity. The remarkable result is that there the semiclassical eigenfunction hypothesis fails, which puts this class of systems into a terra incognita of quantum chaos that should be explored in future work.

We have now given a brief account of the background and the scope of this work. In short, we will discuss questions concerning spectrum, eigenfunctions and dynamics of single-particle systems with chaotic or mixed classical limit. However, it should be understood that we do not attempt to survey the whole work which has been done in this field. The focus will be on motivating and classifying the problems addressed in [A01]–[A11] without repeating in too much detail methods or results presented in this appended material.

1.2 Billiards, maps and graphs

Before we proceed to the problems listed in the previous section we would like to introduce briefly the model systems which we use, namely billiards, Hamiltonian maps and one-dimensional networks (graphs). We have stressed that quantum chaos is concerned with universal properties which do not depend on the type of model considered. Because of this universality it is often very elucidating to pick the simplest model out of the variety of systems sharing the property in question. This is also the strategy we will follow in this work. Quantum chaos provides many examples where results can be generalized to very complex situations, although they were originally obtained thanks to the conceptual, numerical or analytical simplicity of minimal toy models. What is more, the models often became interesting in their own right when experimental realizations were developed. This process has been particularly impressive with billiard systems.

Billiards A billiard is a two-dimensional domain with zero potential. It is restricted by hard walls where specular reflection occurs. Energy is conserved such that the phase space is effectively three dimensional. This is the minimum for chaotic behaviour in continuous systems. Billiards offer a number of properties which simplify their analysis as compared to a general Hamiltonian system. Because of the absence of a potential, trajectories and phase space structures do not depend on the energy, i.e., billiards are scaling systems. As a consequence, time can be replaced by arclength and the billiard dynamics can be understood in an entirely geometric way. Moreover, since the dynamics between two collisions with the boundary is trivial, one can reduce the dynamics to the so-called Birkhoff map [68], which iterates location and angle of subsequent reflections. The calculation of periodic orbits—an important input for semiclassical theories—is often simplified by

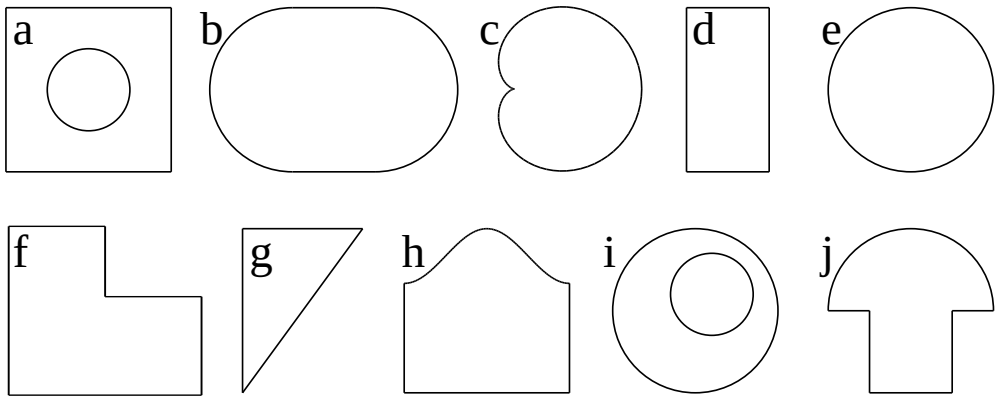

Figure 1.1: Various billiard shapes which are popular models of dynamical systems. (a) Sinai billiard (b) Bunimovich stadium (c) cardioid (d) rectangle (e) circle (f) L-shaped polygon (g) triangle (h) cosine billiard (i) annulus (j) mushroom.

the existence of a symbolic dynamics [69]–[72].

By adjusting the shape of the billiard, virtually any desired dynamical behaviour can be achieved. For some famous examples it can be rigorously proven that the dynamics is completely chaotic. We mention the Sinai billiard [73], the Bunimovich stadium [74] and the cardioid [75]–[77], [72] (Fig. 1.1a-c). Further there are integrable cases like circular or rectangular billiards (Fig. 1.1d,e). Examples for pseudointegrability are provided by triangles and other polygons [78]–[80] (Fig. 1.1f,g). Generic billiards, however, have a mixed phase space which accommodates both regular and chaotic trajectories. Popular examples are the cosine billiard [81, 82] or the (excentric) annulus [83]–[86] (Fig. 1.1h,i). Remarkably, mushroom billiards (Fig. 1.1j) provide a unique example for a system where the border between regular and chaotic dynamics is not fractal and rigorously known [87].

For billiards, the Schrödinger equation reduces to the Helmholtz equation

$$(\Delta + k^2)\Psi(x, y) = 0 \tag{1.1}$$

with $\Delta = \partial_x^2 + \partial_y^2$. The wave number k is related to the energy via $k = \sqrt{2mE/\hbar^2}$. Due to the importance of billiard models, many schemes for a solution of this equation have been developed. The most important ones are the plane-wave decomposition [88, 89], the boundary-integral method [90], the scattering approach [91, 92] and the scaling method [93].

Billiards do also possess a number of specific features which do not immediately generalize to other models of quantum chaos. Some of them are related to the singularity of the potential at the boundary. For example, distortions of the boundary can never be considered as a small perturbation, which excludes in particular the application of the KAM theorem to describe the transition from integrable to chaotic dynamics (say from the circle to the stadium or from the rectangle to the Sinai billiard). In a semiclassical quantization the boundary gives rise to particularly strong contributions from non-classical diffractive trajectories [94]–[97]. And the specific geometry of popular billiard models like the Sinai billiard or the stadium lead to the existence of non-generic families of marginally stable "bouncing-ball" trajectories, which leave distinct traces in the corresponding quantum spectra [98, 99, 81].

There is a huge number of experimental realizations for quantum billiards or systems which are formally equivalent. We mention quantum corrals generated by assembling single-atom walls on the surface of metals [100, 101], 2D electron gases at the interface between different semiconductor materials which can be structured by additional lateral electrodes [27, 28, 30], optical billiards for atoms generated by deflected laser beams [22]–[24], thin microwave resonators which are effectively two-dimensional for sufficiently large wavelengths [33]–[42], microlasers [40]–[42] or vibrating soap films [102].

Also billiards with three spatial dimensions are of interest. However, the relevant experimental realizations by classical fields require usually to consider wavefunctions which are not scalar and Eq. (1.1) has to be modified accordingly, see e.g. [103, 38].

We have relied on billiards as numerical models in [A01, A08] and will use them in Chapters 3 and 4 to illustrate some important concepts.

Hamiltonian maps While chaos in continuous flows requires at least a three-dimensional phase space, the dimensionality can be reduced to two for the dynamics generated by a discrete map. We have already mentioned the Birkhoff map as a way to simplify the study of billiards, and many further examples of two-dimensional maps derived from Hamiltonian systems could be added. However, here we would like to restrict attention to maps which can be explicitly written in a form that is analogous to Hamilton's equations of motion

$$x_{n+1} \;=\; x_n + T'(p_n)$$

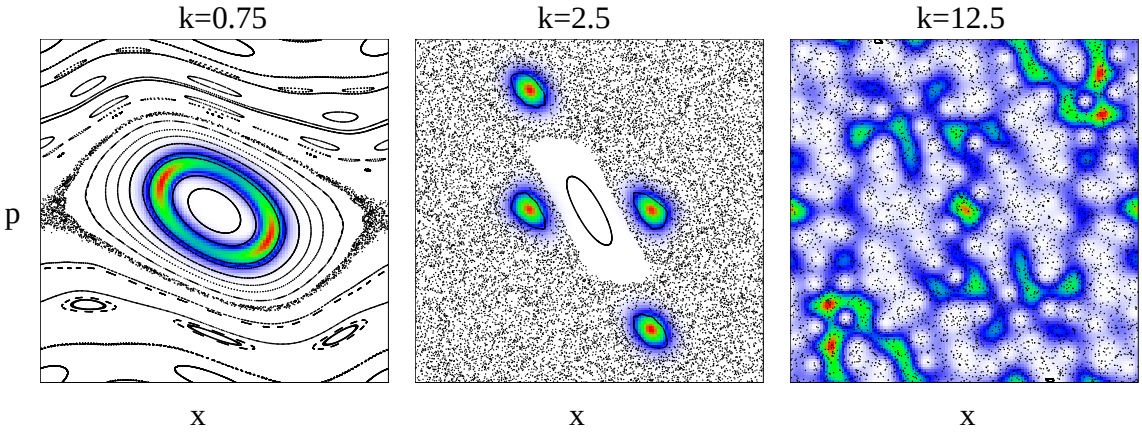

Figure 1.2: The phase space portrait of the kicked rotor (black dots) is compared to the Husimi representation of a selected eigenfunction (colored density) at different values of the kick strength k. Regular and chaotic dynamics coexist in this model. In agreement with the semiclassical eigenfunction hypothesis, the quantum eigenfunctions localize in the semiclassical regime on one of the regular tori (left and middle) or spread uniformly over a chaotic component (right).

$$p_{n+1} \;=\; p_n - V'(x_{n+1})\,. \tag{1.2}$$

We will refer to Eq. (1.2) as a Hamiltonian map. It can be derived from the Hamiltonian of a one-dimensional system which is subject to time-periodic kicks

$$H(p,x,t) = T(p) + V(x) \sum_{n=-\infty}^{+\infty} \delta(t-nT)\,. \tag{1.3}$$

Here, $T(p)$ and $V(x)$ denote the kinetic energy and the potential, respectively. In order to obtain Eq. (1.2) from Eq. (1.3) one defines $x_n = x(t = n+\varepsilon)$ and $p_n = p(t = n+\varepsilon)$ with $\varepsilon \to 0$ as position and momentum immediately after the nth kick.

Because of specific form of the time dependence, the quantization of kicked Hamiltonians is particularly simple and leads to the time-evolution operator

$$\hat{U} = \exp(-\mathrm{i}/\hbar\, V(\hat{x}))\, \exp(-\mathrm{i}/\hbar\, T(\hat{p}))\,, \tag{1.4}$$

describing the evolution of a quantum state from $t = n+\varepsilon$ to $t' = n+1+\varepsilon$. This operator, which is the quantum analogue of the Hamiltonian map (1.2), factorizes into one term depending only on position and a second one

depending only on momentum. In position and momentum representation, respectively, the effect of these factors is just a phase shift. Therefore a very effective scheme to propagate a quantum state is to alternate position and momentum representation by means of a Fourier transformation. This numerical simplicity is the main reason why Hamiltonian maps are frequently used models in quantum chaos.

An important special case of a Hamiltonian map is the kicked rotor with

$$T(p) = \frac{p^2}{2} \qquad V(x) = k \cos x \,, \tag{1.5}$$

leading in Eq. (1.2) to Chirikov's standard map [104]. For increasing kick strength k the phase space of this model changes from completely integrable ($k = 0$) to mainly chaotic and is in general mixed (Fig. 1.2). The kicked rotor has played a major role in the development of quantum chaos, in particular for understanding quantum transport, dynamical localization and spectral statistics for unitary matrices [105].

The dynamics of atoms in time-periodically modulated standing waves of laser light [19, 20] provides the most important experimental realization of the kicked rotator and other Hamiltonian maps.

Although Eq. (1.5) is probably the most famous example of a Hamiltonian map, it is by no means the only possible choice. In fact one may assume virtually any smooth function for $T(p)$ and $V(x)$. Phase space volume is automatically preserved by the special form of Eq. (1.2) and this is the only basic requirement for maps describing Hamiltonian systems. This flexibility allows to "optimize" the classical phase space according to the particular problem one is interested in. We have used this convenient property of Hamiltonians maps in connection with Hamiltonian ratchets in [A10, A11]. Moreover, a modified kicked rotor was used as numerical model in [A01, A08, A09].

Quantum graphs Quantized networks ("quantum graphs") have a long history as models in fields like mesoscopic and molecular physics or quantum computation (see [106]–[109] and Refs. therein) but their connection to quantum chaos has been established only recently by Kottos and Smilansky [110]. The large number of publications extending this pioneering work in a relatively short time clearly demonstrates the virtue of network models in quantum chaos. They concern problems as diverse as scattering and transport [111]–[116], [A03, A06], quantum dynamics [115]–[118], spectral

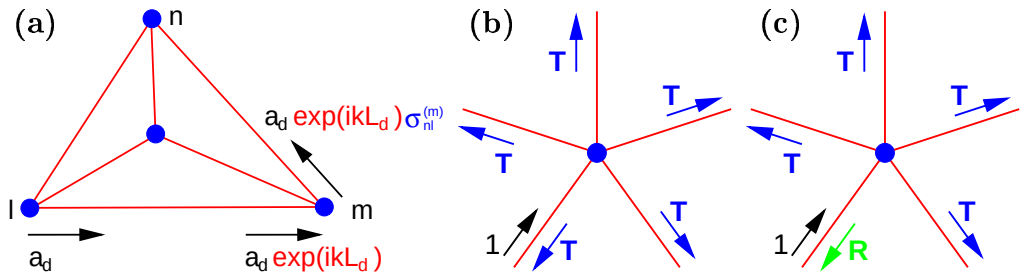

Figure 1.3: (a) illustrates the construction of the bond-scattering matrix with the example of a matrix element describing a transition from a directed bond $d = [l \to m]$ to $d' = [m \to n]$. Upon this transition the amplitude a_d to occupy d is multiplied by a phase from the free propagation along d and by an element of the vertex-scattering matrix at vertex m. (b) and (c) show a single vertex with $v = 5$ attached bonds and DFT or Neumann boundary conditions, respectively. Displayed are the probabilities of all outgoing waves for a wave with unit flux incoming along one of the bonds. For the DFT vertex (b) the probability is equidistributed over the outgoing bonds, each having a share of $T = 1/5$. For the Neumann vertex (c) backscattering is enhanced to $R = 9/25$ while a transition to a different bond occurs only with probability $T = 4/25$.

statistics [119]–[131], [A02]–[A05], properties of wavefunctions [132]–[136], [A07], the numerical modelling of extended systems [A01, A09] and exact quantization of chaotic systems in terms of periodic orbits [137]–[142].

We shall now briefly repeat the formalism for the quantization of graphs. More details can be found, e.g., in [106]. In order to describe a quantum state with fixed wave number k on a graph we need to specify a complex number a_d for each *directed* bond $d = [l \to m]$ leading from vertex l to vertex m. It corresponds to the amplitude of a partial wave propagating in this direction. The *bond-scattering* matrix $S(k)$ is a unitary operator acting on the vector of these amplitudes. It has the matrix elements

$$S_{d',d}(k) = S_{l'\to m',l\to m}(k) = \delta_{ml'}\, \sigma^{(m)}_{lm'}\, \mathrm{e}^{\mathrm{i}kL_{l\to m}}\,. \tag{1.6}$$

The phase factor is due to the free propagation on the bond $d = [l \to m]$ while the other two factors describe the scattering at the vertex m and the transition into a new directed bond d'. This is illustrated in Fig. 1.3a. While the Kronecker δ in Eq. (1.6) simply expresses the fact that a transition from d to d' is possible only if there is a connecting vertex $m = l'$, the vertex-scattering matrix $\sigma^{(m)}$ encodes the scattering properties of this vertex. Pop-

ular choices, referred to as discrete Fourier transform (DFT) and Neumann vertices, respectively, are

$$\sigma_{ln}^{(m)} = \frac{1}{\sqrt{v_m}} \exp(2\pi \mathrm{i} ln/v_m) \tag{1.7}$$

and

$$\sigma_{ln}^{(m)} = 2/v_m - \delta_{ln}\,, \tag{1.8}$$

where $l, n = 1, \ldots, v_m$ denote one out of the v_m bonds attached to vertex m.

The bond-scattering matrix $S(k)$ may be regarded as a discrete-time propagator on the graph, acting on a finite-dimensional Hilbert space of vectors $\mathbf{a}$. This interpretation corresponds to a coarse-grained description of the network, where the propagation along the bonds is not resolved in detail. S is then the analogue to the propagator U for maps, and the wave number k is just a parameter that can be used to generate a statistical ensemble for averaging. However, this parameter is very important as it provides in Eq. (1.6) the rapidly fluctuating phases of matrix elements which are characteristic of the semiclassical regime in more realistic systems. The existence of this parameter is also the main difference to tight-binding models where the Hamiltonian instead of the time-evolution operator is discretized. Although this might look like a minor difference on first sight, it has the consequence that standard tight-binding models are less suitable for investigating quantum chaos or quantum-classical correspondence in general.

The classical system corresponding to the discrete quantum propagator S is obtained after replacing the transition amplitudes by probabilities, i.e., by taking the absolute square of the matrix elements in Eq. (1.6) (see Fig. 1.3b,c). Then the bond-scattering matrix turns into a doubly stochastic matrix which describes a Markov chain on the discrete space of directed bonds. This dynamics is a random walk which is not deterministic and therefore, strictly speaking, not chaotic. However, there is a strong analogy to chaotic systems. In particular, it is possible to define classical (periodic) orbits which are unstable in the sense that the probability to follow a given orbit decays exponentially in time, and there exists a trace formula which is equivalent to the Gutzwiller formula up to the fact that it is exact and not just a semiclassical approximation [106]. This will be made more explicit in Section 2.3.

Quantum graphs can be used to model various types of dynamics by adjusting the topology of the graph and the scattering properties of the

vertices. Random-matrix behaviour is obtained for large and sufficiently well connected graphs with incommensurate bond lengths L_d. Other interesting regimes include, e.g., intermediate statistics for Neumann star graphs [120, 123, 136], diffusion and quantum localization for extended networks with low connectivity [107, 112, 132, A03], or a hierarchical type of dynamics, modelling the chaotic sea in a mixed phases space, which is obtained for chain-like networks with scaling transition probabilities [66, 117]. Moreover, it is possible to generalize the quantization scheme sketched above such that, e.g., relativistic effects and spin dynamics is included [127, 128], and non-standard universality classes are obtained [130, 131].

Despite this flexibility there are also restrictions to the range of problems for which quantum graphs are suitable models. One obvious point is that all orbits in the corresponding classical system are unstable which prevents a direct investigation of generic systems with a mixed phase space.

It should also be mentioned that there are relatively few experiments which can be regarded as a direct implementation of a quantum graph. Some authors have studied properties of light waves in connected networks of optical waveguides [143, 144], and in a recent paper a mechanical analogue based on the vibrations of an elastic disk was suggested [145]. However, in view of the attention quantum graphs have attracted recently, one can hope for more experiments based on, e.g., networks of microwave transmission cables.

We have used quantum graphs as convenient numerical models in [A01, A09] and exploited their analytical simplicity to obtain the results presented in [A02]–[A07].

Chapter 2

Action correlations in semiclassical expansions

2.1 Semiclassical theory of chaotic systems

Arguably the first paper on quantum chaos was written by Albert Einstein in 1917 [146], i.e., even before the modern quantum mechanics was developed. The early quantum theory had established a picture which relied heavily on quantum-classical correspondence and on the integrability of the classical dynamics: the quantum states of the hydrogen atom were postulated to be standing waves on certain classical orbits, selected by the condition that their action integral is quantized. Einstein pointed out that such a prescription must fail for systems where the phase space is not spanned by decoupled pairs of action-angle variables. The problem of quantizing classically nonintegrable systems had been put on the agenda of theoretical physics.

A few years later, in the mid-twenties of the last century, Heisenberg and Schrödinger formulated the modern quantum theory which makes no reference to classical trajectories anymore. Nevertheless semiclassical theories, which strive to express the quantum evolution in terms of purely classical quantities, have always been very important. One reason is that for sufficiently complex quantum systems an exact treatment of the Schrödinger equation is way beyond the available computing power even today. Another and more fundamental reason for the continuing interest in semiclassical theories is the intuitive and analytical *understanding* of the behavior of quantum systems which semiclassics often provides. For quantum chaos this latter as-

pect is clearly dominant, as this field typically deals with low-dimensional systems for which exact quantum computations are not only feasible but even much easier than numerical calculations based on semiclassics.

The most systematic way to obtain a semiclassical approximation to a given quantity starts from the Feynman path integral formulation of quantum mechanics [147]. Integrals over coordinates are performed within the stationary phase approximation (SPA), which is justified when the relevant classical actions are much larger than Planck's constant. The dominant contribution comes then from the vicinity of classical trajectories γ and the result can be cast into the form

$$\sum_\gamma A_\gamma \, \exp\left(\frac{\mathrm{i}}{\hbar} S_\gamma\right) \, , \tag{2.1}$$

where S_γ denotes the classical action along the trajectory and A_γ is a complex normalization prefactor which can also be calculated from classical information only. The precise form of these quantities and the rules selecting the contributing classical trajectories differ according to the application. The most basic semiclassical result in the form of Eq. (2.1) is the van Vleck-Gutzwiller propagator [148]

$$U_{\mathrm{scl}}(x',x'';t) = \sum_\gamma \sqrt{\det\left[\frac{\mathrm{i}}{2\pi\hbar}\frac{\partial^2 R(x',x'';t)}{\partial x' \, \partial x''}\right]} \, \exp\left(\frac{\mathrm{i}}{\hbar} R_\gamma(x',x'';t) - \mathrm{i}\nu_\gamma \frac{\pi}{2}\right) \tag{2.2}$$

which approximates the quantum transition amplitude $\langle x'|\mathrm{e}^{-\mathrm{i}/\hbar \hat{H} t}|x''\rangle$ from x'' to x' in a time interval t in terms of all trajectories γ contributing to this transition classically. In Eq. (2.2) the classical action is $R_\gamma(x',x'';t) = \int_\gamma \mathrm{d}t(\frac{m}{2}\dot{x}^2 - V(x))$ and the Maslov index ν_γ counts the number of conjugate points along γ [59, 60].

From the propagator one obtains an approximation for the energy dependent Green's function $\hat{G}(E) = (E - \hat{H} + \mathrm{i}\epsilon)^{-1}$ $(\epsilon \to +0)$ by a Legendre transformation from time to energy, performed within SPA. The result has again the form of Eq. (2.1),

$$G_{\mathrm{scl}}(x',x'';E) = \frac{1}{\mathrm{i}\hbar} \sum_\gamma \sqrt{\frac{1}{v'_\parallel \, v''_\parallel} \det\left[\frac{1}{2\pi\mathrm{i}\hbar}\frac{\partial p'_\perp}{\partial x''_\perp}\right]} \, \exp\left(\frac{\mathrm{i}}{\hbar} S_\gamma(x',x'';E) - \mathrm{i}\nu_\gamma \frac{\pi}{2}\right) \, . \tag{2.3}$$

The set of contributing trajectories γ is different from Eq. (2.2) as they connect x' and x'' at a given constant energy E while the time is arbitrary. In Eq. (2.3) a special coordinate system is used in which $x_{\|}$ runs along the trajectory while for a system with $d \geq 2$ degrees of freedom the remaining $d-1$ coordinates are subsumed in $x_{\perp}$. The action integral is now $S_\gamma = R_\gamma + Et_\gamma = \int_\gamma p\mathrm{d}q$.

From the semiclassical results Eqs. (2.2), (2.3) one can derive semiclassical expansions in the form of Eq. (2.1) for various other quantities which we can mention only briefly here:

- Gutzwiller's trace formula [59, 60] expresses fluctuations in the density of states of a chaotic system by a sum over all (unstable) periodic orbits. According to the general relation between density of states and Green's function, $d(E) = -\pi^{-1}\mathrm{Im}\,\mathrm{tr}\,G(E)$, it is obtained from Eq. (2.3) by performing an integral $\int \mathrm{d}x\, G(x,x;E)$ within stationary-phase approximation. Half a century after Einstein had posed the problem, this was the solution for the semiclassical quantization problem in fully chaotic systems, although the exponential proliferation of long orbits make the resulting sum divergent. Therefore, even after a lot of work has been invested in developing efficient resummation techniques [149]–[152], the trace formula is of limited virtue for computing individual levels. It is very useful, however, to understand the structure of the spectrum on large scales, as long-range fluctuations are related to a few short periodic orbits of the system.

- Miller developed a formalism for the semiclassical quantization of arbitrary canonical transformations [153], i.e., of basis transformations between two pairs q, p and Q, P of canonically conjugate variables. One special case is given by the dynamical transformations connecting position and momentum at different times. In this case Eq. (2.2) is reproduced by Miller's approach.

- Another important special case of Miller is the scattering matrix of an open system, which quantizes the transformation between the transversal action-angle variables of the asymptotically free motion, i.e., the scattering Poincaré map [154, 155]. In this case the exponent in Eq. (2.1) is the reduced action, namely the action difference between the actual trajectory and a free particle. The contributing trajectories are selected by given values of the asymptotically conserved action variables

(including energy in conservative systems) before and after the scattering.

- Particularly important scattering geometries are cavities (billiards) connected to two waveguides. Of interest is the subblock of the scattering matrix describing the transmission, because physically relevant quantities like conductance and shot noise for phase-coherent electron transport can be derived from it. Semiclassically, elements of this transmission matrix are given by a sum over scattering trajectories connecting the two attached waveguides [156, 157].

- An important alternative route to the trace formula goes via a semiclassical expansion of Bogomolny's transfer operator [150, 158]. This operator $T(E)$ is the quantization of a Poincaré section through a closed system and the quantization condition is a secular equation of the form $\det(I - T(E)) = 0$. Semiclassically, the transfer operator is given by a sum (2.1) over trajectories starting and ending on the surface of section. If this surface is chosen suitably, only few trajectories contribute.

- In a modification of this approach by Smilansky et al. [91, 92] the transfer operator is replaced by the scattering matrix of an auxiliary scattering system. The unitarity of this matrix is one advantage, another one is the very illuminating connection between spectral and scattering properties.

For our purpose, expansions in the form of Eq. (2.1) are the principal semiclassical tool, although they are not the only possible approach. For example, while the large number of trajectories contributing to Eq. (2.1) in a chaotic system can make this expansion unsuitable for numerical calculations, there exist very efficient numerical schemes for the semiclassical propagation of complex quantum systems which are based on Heller's variational wavepacket dynamics [159, 160].

2.2 Quantum two-point correlations

With the exception of the density of states, the quantities discussed in the previous section are complex amplitudes which are not directly measurable.

Of physical interest are typically the associated probabilities, i.e., the absolute squares of these amplitudes: $|U(x', x'', t)|^2$ is the probability for a quantum transition from x'' to x' in time t, the modulus squared of a scattering matrix element is a partial cross section, the sum of the absolute squares of the transition matrix elements gives the Landauer-Büttiker conductance etc. Because of their structure, we can refer to all these quantities as quantum two-point correlation functions. The main goal of the present chapter is a semiclassical theory of such two-point correlations.

The form factor The paradigmatic example of a two-point correlator is the spectral form factor. It is defined as the smoothed Fourier transform of the autocorrelation function of the quantum density of states. Equivalently, $K(t)$ can be represented in terms of the propagator $U(t) = \exp(-\mathrm{i}Ht/\hbar)$ as

$$K(t) = \frac{1}{N}\langle |\mathrm{tr}U(t)|^2 \rangle \,, \tag{2.4}$$

and in this form it has the interpretation of an averaged quantum probability to return after time t to the initial state. To evaluate Eq. (2.4) from the energy spectrum, one considers a spectral window $[E_n, E_{n+N}]$ which is small compared to classically relevant energy scales but contains many states, $N \gg 1$. The effective propagator $\tilde{U} = \sum_{i=n-N/2}^{n+N/2} |i\rangle \, \mathrm{e}^{-\mathrm{i}tE_i/\hbar} \, \langle i|$ is then a finite matrix. The average $\langle \ldots \rangle$ is taken over the energy E_n or some external parameter of the system. For example, the data shown in Fig. 2.4a were obtained by averaging over 1,187 energy levels of a quarter Sinai billiard in groups of $N = 32$ (cf Fig 10b of Ref. [A01]). For Fig. 2.4b the kicked rotor with $N = 64$ was averaged over kicking strengths $k \in [12.5, 15]$, and for Fig. 2.4c the bond-scattering matrix of a DFT star graph with $N = 64$ arms was substituted in Eq. (2.4) and the average was over the wavenumber $0 \leq k < \infty$.

To interpret the result of Fig. 2.1 we note that in the absence of correlations between different eigenvalues the form factor is the Fourier transform of a δ-shaped correlator, i.e., it is constant $K(t) = 1$. The deviation from unity observed at small times is therefore the signature of correlations between quantum levels (the "correlation hole"). Such correlations appear on energy scales of the order of the mean level spacing Δ and greater and therefore on time scales up to the Heisenberg time

$$t_{\mathrm{H}} = 2\pi\hbar\Delta^{-1} \,. \tag{2.5}$$

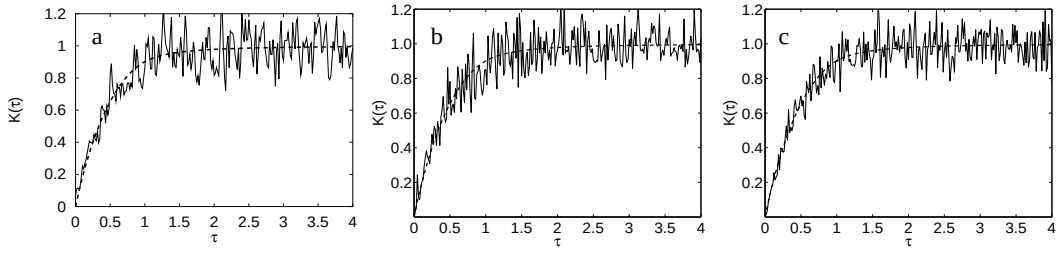

Figure 2.1: The form factor Eq. (2.4) for (a) the Sinai billiard, (b) the kicked rotor and (c) a DFT star graph is compared to the RMT result Eq. (2.8) (smooth curves). τ is the time in units of the Heisenberg time Eq. (2.5).

From Fig. 2.1 we see that the form factors of completely different systems coincide, if time is measured in units of the Heisenberg time

$$\tau = t/t_{\rm H}\,. \tag{2.6}$$

This is one instance for the universality of spectral fluctuations mentioned in the introduction. It persists in all chaotic systems as long as the Heisenberg time is the only relevant time scale.

Random-matrix theory Within RMT one extends the average in Eq. (2.4) to an ensemble average over *all* unitary matrices U, irrespective of the specific system for which the form factor is required. The resulting ensemble is called the CUE. Alternatively one may replace the Hamiltonian H by a member of the GUE, which contains all Hermitian matrices. The result is the same in the limit $N \to \infty$ and equal to

$$K_{\rm CUE}(\tau) = \begin{cases} \tau & \tau < 1 \\ \quad \text{for} & \\ 1 & \tau > 1 \end{cases}\,. \tag{2.7}$$

If time-reversal symmetry is present, one restricts the random-matrix ensemble to all symmetric unitary matrices (COE) or all real Hermitian matrices (GOE), respectively, and obtains instead

$$\begin{aligned} K_{\rm COE}(\tau) &= \begin{cases} 2\tau - \tau\,\ln(2\tau+1) & \tau < 1 \\ \quad \text{for} & \\ 2 - \tau\,\ln\frac{2\tau+1}{2\tau-1} & \tau > 1 \end{cases} \\ &= 2\tau - 2\tau^2 + 2\tau^3 + \ldots \qquad (\tau < 1/2)\,. \end{aligned} \tag{2.8}$$

Fig. 2.1 demonstrates the numerical fact, that the form factor of chaotic systems follows these predictions of RMT very well as long as no system-specific properties are important. However, despite all numerical evidence showing that quantum spectral statistics of chaotic systems agrees with RMT [50], [1]–[9] and despite a lot of work towards an analytical justification of this conjecture [161]–[163], the universality is not yet understood in detail. In other words, it is not yet completely clear to which properties, to what extent and precisely under what conditions RMT predictions do apply.

The diagonal approximation One possible approach to answer these open questions concerning the applicability of RMT is a semiclassical theory for two-point correlation functions. Taking the absolute square of a semiclassical expansion in the form of Eq. (2.1) one obtains a *double sum* of classical trajectories

$$\left| \sum_{\gamma} A_\gamma \, \exp\left(\frac{\mathrm{i}}{\hbar} S_\gamma\right) \right|^2 = \sum_{\gamma\gamma'} A_\gamma A_{\gamma'}^* \, \exp\left(\frac{\mathrm{i}}{\hbar}[S_\gamma - S_{\gamma'}]\right) . \tag{2.9}$$

The problem is now to find a method that allows to perform the summation over γ, γ' analytically.

Until recently, the only such method was Berry's diagonal approximation [61], where one keeps only the terms for which γ, γ' denote the same trajectory or a pair of trajectories related by an exact symmetry such as time reversal. To justify this approximation one notes that for these terms the phases in Eq. (2.9) cancel exactly, $S_\gamma = S_{\gamma'}$, while for other pairs γ, γ' a phase difference remains that is rapidly fluctuating in the semiclassical limit $\hbar \to 0$. Therefore, an average over the energy or some control parameter as in Eq. (2.4) is expected to remove these terms. For $\hbar \to 0$ the size of the necessary averaging interval vanishes on any classical scale such that classical quantities like the amplitudes A_γ are effectively constant. Within the diagonal approximation these amplitudes combine to the classical probability $P_\gamma = |A_\gamma|^2$ of the trajectory and one obtains a sum in the form of $\sum_\gamma P_\gamma$ which can be evaluated using classical sum rules for periodic orbits [164, 165].

For example, the semiclassical result obtained for the spectral form factor in this way is [61, 166]

$$K_{\mathrm{scl}}(\tau) = \gamma\tau \, P_{\mathrm{cl}}(\tau t_{\mathrm{H}}) \tag{2.10}$$

where $\gamma = 1$ in the absence of symmetries and $\gamma = 2$ for systems invariant under time-reversal. $P_{\mathrm{cl}}(t)$ is the averaged classical probability to return in

phase space. It is normalized such that $P_{\rm cl}(t \gg t_{\rm erg}) = 1$ after the time scale $t_{\rm erg}$ for the decay of classical correlations.

For the case where this time is negligible compared to the Heisenberg time, $t_{\rm erg} \ll t_{\rm H}$, one obtains the original result of Berry

$$K_{\rm scl}(\tau) = \gamma\tau\,. \tag{2.11}$$

For $\gamma = 1$ and $\tau \leq 1$ this is precisely the RMT result Eq. (2.7), while for $\gamma = 2$ only the leading order in the small-τ expansion (2.8) is reproduced. In either case we see that the diagonal approximation is applicable for short times only and misses, in particular, the saturation of the form factor beyond the Heisenberg time, $K(\tau \gg 1) = 1$ (Fig. 2.1). Berry compensated for this drawback by a separate (not semiclassical) argument, showing that no correlations persist after the Heisenberg time. This leads to

$$K(\tau) = 1 \qquad (\tau \gg 1)\,, \tag{2.12}$$

and connecting the functions (2.11) and (2.12) at their intersection point $\tau = \gamma^{-1}$ he obtained a complete approximation to the form factor (which happens to be exact for systems without time-reversal invariance).

Non-universal systems We have applied the outlined semiclassical theory for the spectral form factor in situations which are interesting and challenging because of non-universal features in the classical dynamics [A01], [A08]–[A10]. Then neither Berry's result nor RMT is directly applicable. Deferring spatially extended systems [A08]–[A10] to Chapter 4 we discuss here only a simple example, namely a completely chaotic system consisting of two identical, weakly connected cells (see Fig. 1b of [A01]). In this case the following modifications of Berry's approach were necessary:

(i) γ in Eq. (2.10) contains a factor 2 irrespective of the presence or absence of time-reversal invariance since almost all periodic orbits of the system form a pair of two symmetry-related partners.

(ii) Since the cells are weakly connected, the classical equilibration between them follows an exponential law with a large time constant. Therefore the classical return probability in Eq. (2.10) is given by $P_{\rm cl}(t) = 1 + {\rm e}^{-t/t_{\rm erg}}$.

(iii) The long-time behavior is non-trivial in this case. We derived an approximation, Eq. (52) of [A01], which contains a free parameter in contrast to Eq. (2.12).

(iv) This parameter can be determined by matching at the Heisenberg time $\tau = 1$ the long-time behavior to the semiclassical expression Eq. (2.10). The matching works well, in cases without time-reversal invariance, as numerical studies for the kicked rotor confirm (Fig. 13 of [A01]). In presence of time-reversal symmetry, however, the diagonal approximation is insufficient to describe the form factor correctly up to $\tau = 1$, similar to the case of Eq. (2.11) above, and the free parameter of the long-time dynamics cannot be determined semiclassically.

To summarize this part, the strength of the semiclassical theory of two-point correlators such as the form factor is its potential to account for individual properties of the specific system at hand. This information would be lost in a random-matrix approach. The weakness of the semiclassical theory is that the diagonal approximation fails after a short initial time. A semiclassical theory which avoids the diagonal approximation is therefore a very important goal.

2.3 Consequences of action correlations

The reason for the failure of the diagonal approximation are correlations between the actions of different classical trajectories or periodic orbits $\gamma \neq \gamma'$. Because of these correlations there are terms in Eq. (2.9) for which the action difference is nonzero but almost constant with respect to variations in the energy or some other parameter. Then these terms cannot be removed by averaging and lead to deviations from the diagonal approximation. This was anticipated already by Berry [61] and subsequent work [167, 168] revealed details about the precise nature of the correlations. In particular, it was found [168] that there exist families in which the orbits are correlated while no correlations exist between different families. However, these insights did not immediately lead to a scheme for calculating the effect of the correlations analytically. For this purpose it is very useful to have a model system with (i) a simple symbolic dynamics which allows to enumerate the classical orbits γ and (ii) simple and explicit expressions for the corresponding actions S_γ

and stability amplitudes A_γ. Such a model system is provided by quantum graphs.

Action correlations in graphs As discussed in Section 1.2, the bond-scattering matrix S on a graph can be interpreted as discrete time-evolution operator. Then the amplitude for a transition between two directed bonds in time t is given by a matrix element of S^t. It can be represented in the form of Eq. (2.1) as a sum over sequences of $t+1$ connected bonds $\gamma = [\gamma_0, \ldots, \gamma_t]$, i.e., as sum over the trajectories on the graph,

$$(S^t)_{d'd''} = \sum_{\gamma:\ \begin{subarray}{l}\gamma_0 = d'' \\ \gamma_t = d'\end{subarray}} A_\gamma \mathrm{e}^{\mathrm{i}kL_\gamma} \,. \tag{2.13}$$

Here the total length of the trajectory is $L_\gamma = L_{\gamma_0} + \ldots + L_{\gamma_{t-1}}$ and the stability amplitude is the product of all the elements of vertex-scattering matrices σ encountered along γ. Inserting this expansion into Eq. (2.4) and performing an average over k we obtained an expression for the form factor in which the above-mentioned family structure is explicitly present (Eq. 35 of [A02]): Correlated are orbits which have the same lengths because they traverse the same set of bonds with the same multiplicity (but different itinerary). An example for such a family of isometric orbits is shown in Fig. 2.2.

This structure of the families of correlated orbits can be generalized from graphs to other systems: a family is formed by those orbits which traverse the same phase-space regions in different order or, if a symbolic dynamics exists, whose code is formed by permutations of the same subsequences (see, e.g., [169] for the example of the Baker map). In this sense we can regard quantum graphs as generic models for the study of action correlations. At the same time, they have a number of convenient specific properties which considerably simplify all explicit analytical calculations.

Due to these simplifications we were able to perform the summations in Eq. (2.1) analytically and without any approximation for some very simple graphs and thus succeeded for the first time to obtain the correct quantum two-point correlations from classical trajectories. Specifically we calculated in [A02] the complete form factor for a graph with a single non-trivial vertex (a star graph with two arms, Fig. 2 of [A02]). It is worth noting that even for this simple model the calculation is quite complex and lead to proofs

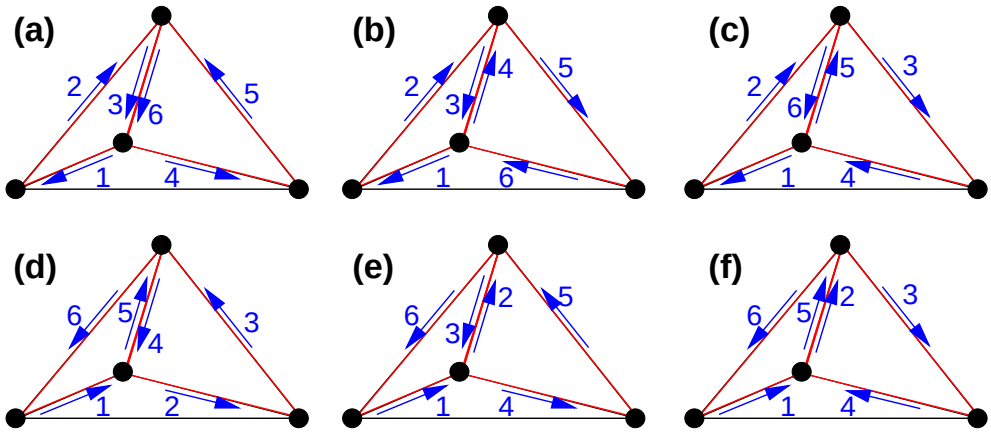

Figure 2.2: A complete family of six isometric orbits on a fully connected undirected graph. Arrows indicate the direction of the orbit and numbers give its itinerary. The orbits (a), (f), e.g., are connected by time-reversal and this pair is therefore counted in the diagonal approximation. For other orbit pairs inside the family such as (a), (b) or (a), (c) there is no simple transformation relating the partners and yet their lengths are identical. (a), (b) is an example for a Sieber-Richter pair of orbits: these orbits are composed of two loops and one of the loops is traversed with opposite orientation in the two partner orbits.

for some previously unknown combinatorial identities (see Eqs. (60)-(66) of [A02]). They represent an unexpected and interesting link between quantum chaos and combinatorics [122].

Further we calculated in [A03] the quantum return probability $P(t) = |\langle i|U^t|i\rangle|^2$ for a chain-like graph with random bond lengths and random vertex-scattering amplitudes. Again the calculation was based on an expansion in the form of Eq. (2.9) and did not involve any approximation. By showing that $P(t \to \infty)$ approaches a positive constant we were able to proof Anderson localization within periodic-orbit theory for the first time.

Our approach to two-point correlations was applied by various authors in other types of quantum graphs [170, 119, 121, 138, 171]. However, it does not come as a surprise that the range of models allowing for exact results is limited. In order to make further progress one needs approximation methods that can account for action correlations in more general situations.

Sieber-Richter pairs An important step towards a semiclassical theory of two-point correlations was taken in the recent work of Sieber and Richter [172]–[174]. They considered the problem of weak localization, that is higher-order corrections in two-point correlations which are due to time-reversal invariance. An example are the nonlinear terms in the expansion of the spectral form factor Eq. (2.8). They observed that the leading order correction $-2\tau^2$ is already reproduced from a small subset of correlated orbits, namely those in which the partners forming a pair differ only in the orientation of a single loop (see Fig. 2.2a, b for an example). Based on this idea, they calculated analytically the leading-order correction to the spectral form factor [173], and later the leading-order correction to the conductivity [174], in the Hadamard-Gutzwiller model (a uniformly hyperbolic billiard on a surface of constant negative curvature). In both cases agreement with RMT predictions was found.

Later the method was applied in more general situations and considerably extended [175]–[180], [128, 129]. For quantum graphs we derived in [A04] a sufficient condition on the classical dynamics (Eq. (4) of [A04]) which guarantees that the result of adding all Sieber-Richter pairs agrees with the leading-order correction in Eq. (2.8). And we were also able to reproduce for the first time the cubic term in this expansion from periodic orbits [A05].

Beyond weak localization effects The existence of Sieber-Richter pairs is dependent on time-reversal symmetry because only then part of a trajectory (one of the two loops) can yield in either orientation the same action contribution. On the other hand, also in systems without time-reversal invariance interference effects between correlated classical trajectories can be very important.

The relevant trajectories can be found by an extension of the approach of Sieber and Richter: one considers a trajectory which is composed of a certain number of long segments and permutes their order. As the partners generated in this way follow each other along the segments and differ only in relatively short crossing regions, their actions are correlated. The relative importance of the correlations diminishes with increasing number of segments and crossing regions, i.e., for a calculation to leading order it is sufficient to consider trajectories which consist of few segments.

On this basis we have demonstrated in [A06] that, within the semiclassical approach, certain action correlations are responsible for shot noise (temporal fluctuations in the current through a device due to the discreteness of the electron charge). In contrast to weak localization, these correlations involve four instead of just two classical trajectories (Fig. 2 of [A06]). We have explicitly calculated the effect of these correlations in a quantum graph modelling a quantum dot with perfect coupling to two electron waveguides (Fig. 1 of [A06]) and found agreement with the corresponding random-matrix prediction. It is worth noting that in the case of shot noise, action correlations are no small correction to the diagonal approximation. Rather they yield the leading-order result.

In a more recent study [118] we have also related quantum corrections in *dynamical* quantities, such as the probability to survive inside an open system, to the presence of certain trajectory pairs with correlated actions. Again quantum graphs were used as model system.

It can be expected that further applications of action correlations will be found and that those examples which are so far restricted to quantum graphs [A06, 118] will be generalized using the methods developed for weak localization [175]–[180]. Nevertheless some fundamental open problems do remain. First and foremost it would be desirable to have a complete semiclassical description of two-point and higher order correlations, e.g., to obtain the full series in Eq. (2.8) instead of just one or a few leading-order terms. Equally important is a semiclassical theory for action correlations in systems with non-universal classical features such as the examples described in Sections

2.2 and 4.1. Up to now, almost all results obtained semiclassically beyond the diagonal approximation simply reproduce the RMT behavior or were restricted to very special models like star graphs [A02, 170, 119]. However, only in a non-universal situation, where the result does not coincide with the RMT prediction anyway, a semiclassical theory provides new results and is therefore indispensable.

Chapter 3

Strong scarring on classical periodic orbits

We come now to one of the most direct manifestations of chaotic classical dynamics in a quantum system, namely the scar phenomenon [181]–[198]. A scar is a quantum eigenfunction with excess density near an unstable classical periodic orbit. Such states are neither expected within RMT [53] nor within Berry's random plane wave model [63], which predict that chaotic wavefunctions must be evenly distributed over phase space, up to quantum fluctuations. What is more, the Shnirelman quantum ergodicity theorem [199] proofs that in the semiclassical limit of a completely chaotic system almost all eigenfunctions have this property in a certain mathematical sense. This was confirmed and qualified by many studies of wave functions in chaotic systems [200]–[205]. However, exceptionally scarred states are possible and were also observed in numerical simulations [195]–[198]. For illustration we show in Fig. 3.1 two eigenstates of the cardioid billiard [90]. Fig. 3.1a shows a typical state: the probability density to find the quantum particle at a certain position fluctuates with a wavelength corresponding to the energy of the state, but no other global structure is visible. The state is essentially equidistributed over the available space. In contrast, the scarred state of Fig. 3.1b is strongly enhanced along a periodic orbit of the billiard.

Even though such states are rare they can have important consequences, as experimental evidence and applications of scars in systems as diverse as microwave resonators [35, 206], quantum wells in a magnetic field [190], Faraday waves in confined geometries [192], open quantum dots [190, 191] and semiconductor diode lasers [193, 194] show.

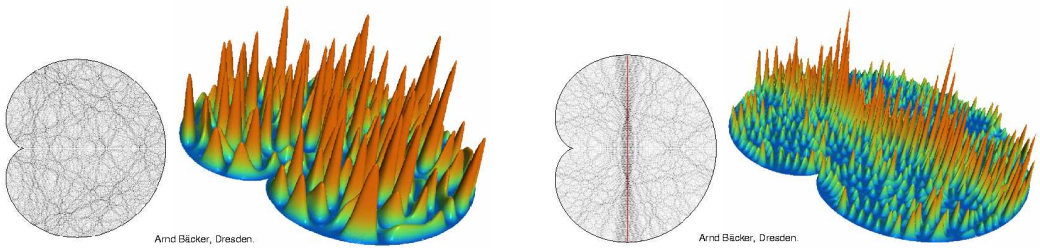

Figure 3.1: The probability density of two eigenstates of the completely chaotic cardioid billiard is shown with both, a gray scale and a coloured surface plot. While the left state is essentially equidistributed over the whole billiard area, the right example is strongly scarred by the periodic orbit shown with a red line. The figure is courtesy of A. Bäcker [90].

In these experiments, scarring is a property of *individual* eigenstates, clearly visible to the eye when the state is plotted as, e.g., in Fig. 3.1. This is also the way in which scarring was discovered in the first place: some eigenstates of the stadium billiard (Fig. 1.1b) showed an unexpected clear structure which was easily associated with classical periodic orbits. On the other hand, the first semiclassical theory of scarring developed by Heller in his seminal paper of 1984 [181] predicts only that within certain groups comprising many eigenstates an enhanced localization must exist *on the average*. This is a priori a different phenomenon. Typically, enhanced wavefunction localization due to the presence of short unstable orbits can be detected statistically although scarring in any particular state of the ensemble is much too weak to be visible. For the discrimination of these two different types of scars the terms *weak* and *strong scarring* are used.

Starting from Heller's original ansatz the understanding of weak scarring has been developed into a very detailed theory [188]. The main idea is to connect localization properties of eigenfunctions to the dynamics of the system, in particular to the return probability of a quantum state $P(t) = |\langle\psi|\hat{U}(t)|\psi\rangle|^2$. It can be argued that the short-time dynamics ($t \ll t_{\mathrm{H}}$), approximated semiclassically with a few periodic orbits, provides sufficient information to estimate the long-time average of this quantity which in turn is nothing but the mean inverse participation number of the eigenstates in the test state $|\psi\rangle$, i.e., the standard measure of eigenfunction localization.

Unfortunately it is very hard to apply this line of argumentation to strong scarring. In order to describe single eigenfunctions one needs precise infor-

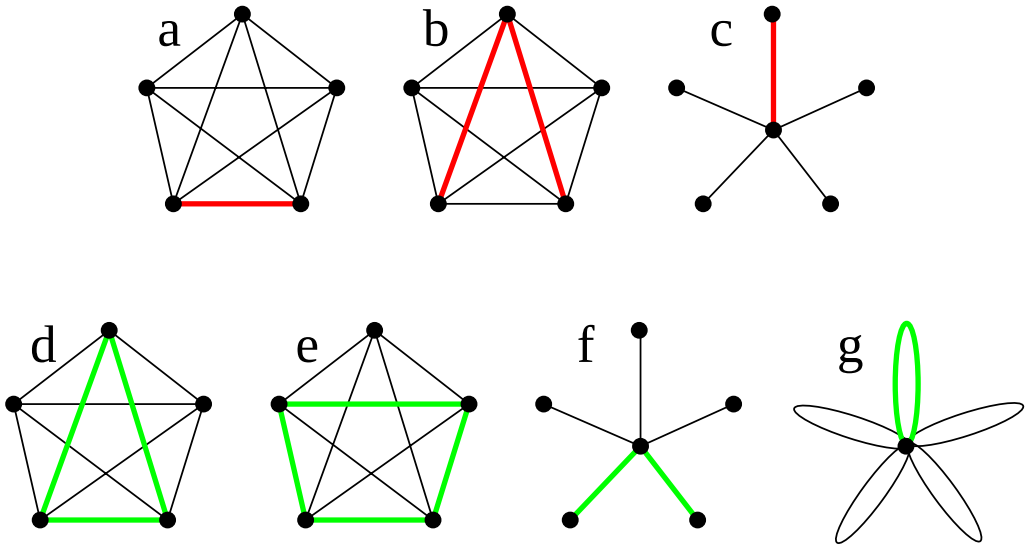

Figure 3.2: Periodic orbits supporting strong scars in quantum graphs are selected by a topological criterion: the orbit must not be reflected at a vertex unless the valency of the vertex is one [A07]. The upper row shows three cases (a)-(c) which are excluded by this criterion. The lower row shows orbits (d)-(g) which do support scars. Notably the shortest orbits bouncing back and forth between two adjacent vertices are excluded for (a) fully connected and (c) star graphs. For star graphs the shortest scarring orbits are shown in (f). Orbits with the same shape are excluded, however, for fully connected graphs (b).

mation about the dynamics of the system at least up to the Heisenberg time t_{H}, Eq. (2.5), because only then the discreteness of the quantum spectrum can be resolved. Because of their exponential proliferation this requires to sum over huge sets of classical orbits. Implementing periodic orbit resummation techniques, scarring can indeed be predicted numerically for individual states and from classical information only [185]–[187]. Nevertheless, with this scheme one can at most hope to reproduce exact quantum computations numerically; no further analytical insight can be obtained in this way.

Thus, with the exception of some very recent results [189, 135, 136], little is known about the nature of strong scarring. It is tempting to regard weak and strong scarring as essentially the same phenomenon, and in fact this assumption is tacitly made in many publications on the subject. However, in the appended paper [A07] we have studied this question for quantum graphs and reached the opposite conclusion: *strong and weak scarring are completely*

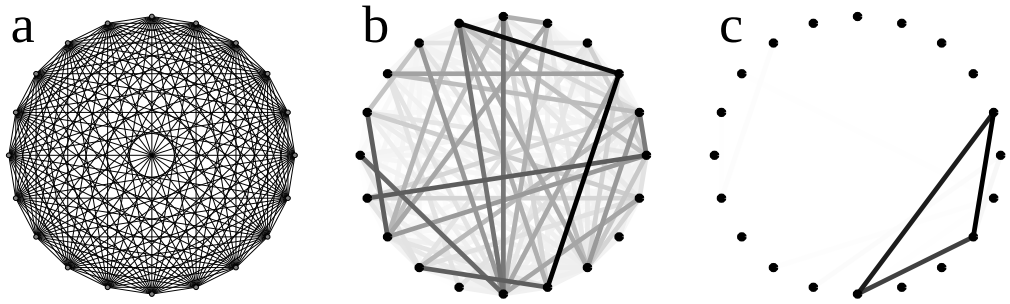

Figure 3.3: A fully connected graph with $V = 20$ vertices and $B = 190$ (undirected) bonds is displayed in (a). Two eigenstates are shown in (b) and (c) by selecting the colour for each bond according to the intensity of the state (white corresponding to zero, black to maximum). The state (b) is representative of the vast majority of eigenstates which spread over the graph without any pronounced structure. In contrast, the scarred state (c) is concentrated almost completely on three bonds forming a triangle.

unrelated. In particular they lead to localization on different periodic orbits and leave distinct traces in statistical localization measures such as the distribution of inverse participation numbers.

These conclusions are based on a theory predicting for graphs with Neumann boundary conditions the orbits which support strong scars, the energies at which strong scars occur and the statistical distribution of scarring intensities, see Eqs. (7), (9) and (12) of [A07]. Remarkably, our criterion for scarring orbits is based on topological information only and does not involve the classical stability of the orbit. For example Fig. 3.2 shows in the upper row three configurations (a)-(c) where no strong scars can exist while the orbits (d)-(g) in the lower row do support scars. Although the periodic orbits bouncing back and forth between two adjacent vertices are by far the least unstable ones they are excluded from scarring in fully connected graphs (a) and star graphs (c). This is in sharp contrast to weak scarring. Kaplan [132] has shown that the theory of weak scarring outlined above does apply to quantum graphs. One can conclude from it that the least unstable orbits must have the strongest influence on eigenfunction localization. The reason is that classical trajectories can cycle in their vicinity for a relatively long time and thereby increase the return probability beyond the ergodic average. This effect is also visible in eigenfunctions statistics of quantum graphs (Fig. 1 of [A07]). Enhanced localization in the majority of the states, resem-

bling Fig. 3.3b, can be explained semiclassically using the shortest orbits of the system only, but none of the states shows any pronounced scarring on these orbits. On the other hand, the scarred state Fig. 3.3c is concentrated on a triangular periodic orbit which is highly unstable but selected by our topological criterion (Fig. 3.2d).

We would like to stress that with our approach we circumvent the above mentioned problem of predicting the long-time dynamics of the system from periodic orbits although we do describe individual eigenstates. This is possible because we do explicitly use the information that the states in question are quantized, $S|\phi\rangle = \mathrm{e}^{\mathrm{i}\theta}|\phi\rangle$. Then it turns out to be sufficient to consider the quantum propagator S for very short times ($t = 1, 2$), which is easily done in terms of just a few classical trajectories. The implementation of this idea is greatly facilitated by the analytic simplicity of quantum graphs and therefore it is at the moment not clear if and how our scar theory can be generalized to other systems. However, it is interesting to notice the analogy of our ansatz to the argumentation establishing in [A11] the existence of amphibious eigenstates in disordered Hamiltonian ratchets. One can hope that also in other situations new insights into the structure of eigenstates can be gained from a combination of explicit quantization with short-time semiclassics, possibly including quantum corrections as those discussed in Chapter 2.3.

Chapter 4

Quasi-1D system with spatial periodicity

In the present chapter we turn our attention to extended, spatially periodic systems. They are ubiquitous in nature and the physically most important questions concern their transport properties. A prominent paradigm comes from solid state physics, where the connection between the atomic structure of crystalline materials and the conductivity of electrons or heat are a topic of research. However, atomic or molecular crystals are at most marginally related to quantum chaos because for these systems one is normally interested in the deep quantum regime where only one or a few energy bands are occupied. In this situation the classical limit of the system is hardly relevant.

More interesting from our point of view are potentials with *mesoscopic* spatial periods, of the order of ten to a few hundred nanometers. Examples include electronic transport through artificial crystals in semiconductor nanostructures (antidot lattices) [207, 208], semiconductor ratchets [209, 210] or the dynamics of cold atoms in optical potentials created by a laser beam [19, 20], i.e., precisely those situations where billiards and quantized maps are relevant models. Under suitable experimental conditions long decoherence times are possible and quantum effects remain important although many levels contribute to the dynamics. Then the classical phase space leaves very distinct traces in the quantum transport properties which we will address in this section.

4.1 Diffusive systems with spatial periodicity

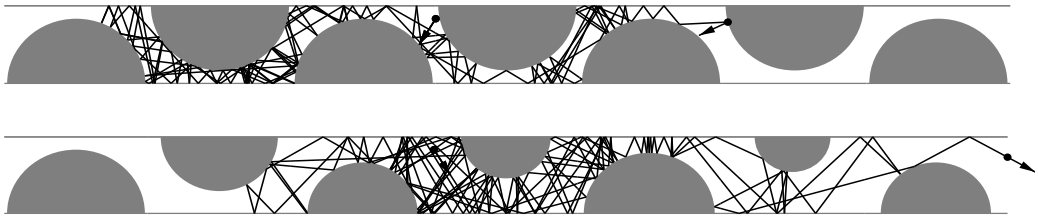

Figure 4.1: The Lorentz gas is an example for an extended chaotic system with normal classical diffusion. It represents a single point particle scattered by circular obstacles which are arranged (a) in a periodic and (b) in a disordered geometry. Normal classical diffusion results in either case as long as the particle has a finite horizon, i.e., as long as a finite distance between successive collisions with the obstacles is guaranteed.

Chaotic dynamics in extended Hamiltonian systems usually leads to diffusion on large spatial scales. It is important to realize that no randomness in the dynamics is required for this behavior, neither stochastically fluctuating forces as in the case of Brownian motion nor spatial disorder which is frozen in time. Classical chaos is sufficient for diffusive transport since it leads to the decay of all correlations, including a randomization of the velocity in the course of time. As an illustration, Fig. 4.1 shows the Lorentz gas (a spatially extended version of the Sinai billiard).

In such a situation, the distribution of an ensemble of classical particles which were initially well localized in space remains symmetric around the initial position, $\overline{x}(t) = \text{const.}$, and has a width growing with time as a power law. Fully chaotic dynamics with exponentially decaying correlations leads to normal diffusion $\Delta x = Dt$, and in the present section we will concentrate on this typical case.

While for the classical transport the presence of spatial periodicity is immaterial, quantum transport depends crucially on it. Periodic systems have a band spectrum, and under very general conditions this leads to ballistic transport for large times, $\Delta x \sim t^2$. On the other hand, in disordered systems one finds Anderson localization such that asymptotically there is no quantum transport, $\Delta x = \text{const}$. While transport theory for disordered systems is a very well developed field [7]–[9], [55]–[58], not so much is known about the

scenario, where spatial periodicity and classical diffusion are simultaneously present. In [A08] we have applied the semiclassical theory of spectral two-point correlations (Section 2.2) to the band spectra of periodic, classically chaotic systems (see Fig. 3 of [A08] for an example of such a spectrum).

However, in this case the form factor Eq. (2.4) is of limited significance because in its definition no information about the band structure of the spectrum is preserved. It is possible to project the propagator U onto the subspace of a given Bloch phase θ, but direct substitution of U_θ into Eq. (2.4) does not yield any information about correlations in the spectrum for different values of θ. In order to account for such correlations, which are important for describing quantum transport, we generalized the form factor to

$$K_n(t) = \frac{1}{N}\langle |U_n(t)|^2 \rangle \tag{4.1}$$

[A08]. U is here replaced by the Fourier transform of the symmetry-projected propagator

$$U_n(t) = \frac{1}{2\pi}\int_0^{2\pi} \mathrm{d}\theta\, e^{-\mathrm{i}\, n\theta} U_\theta(t) \tag{4.2}$$

or the discrete analogue of Eq. (4.2) for a system with a finite number of identical unit cells. For $n = 0$ Eq. (4.1) reduces to the normal form factor Eq. (2.4). While the latter one has the interpretation of a quantum probability to return to the initial state and in particular to the initial unit cell, $K_n(t)$ describes transitions which span n unit cells in time t, i.e., n/t has the interpretation of a velocity. Indeed it can be shown that for for long times, $t \to \infty$, $K_n(t)$ is proportional to the the probability of finding a Bloch state with velocity expectation value $v = n/t$ [211]. This underlines the connection between quantum transport and the spectral information contained in the generalized form factor.

Within the diagonal approximation the generalized form factor can be expressed in terms of the periodic orbits of a single unit cell on a cylinder, i.e., with periodic boundary conditions. The index n is given by the winding number of the orbit, which counts how often the obit encircles the unit cell before it closes onto itself. Each such winding corresponds in the extended system to a transition into the next unit cell. The sum over all classical orbits with winding number n gives a discretized classical propagator $P_n(t)$ and in analogy to Eq. (2.10) we find

$$K_n(\tau) = \gamma_n \tau P_n(\tau\, t_\mathrm{H})\,. \tag{4.3}$$

γ_n counts here the degeneracy of orbits in the extended system which is for almost all orbits given by the total number of unit cells. For large time t the classical dynamics is diffusive and $P_n(t)$ can be approximated by a Gaussian with width Dt such that finally an explicit semiclassical expression for the generalized form factor can be given which depends only on the diffusion constant D (Eq. (10) of [A08]). As in Section 2.2 this semiclassical result is valid for short times only and is complemented by a separate expression for the long-time behavior which essentially describes simple ballistic spreading due to the underlying band structure of the spectrum. By matching both expressions at the Heisenberg time a complete semiclassical theory for the generalized form factor is obtained which compares favourably to RMT results and numerical data (Figs. 2, 4 of [A08]).

This theory can be extended such that also the transition from exact periodicity to weak disorder can be described [A09]. Upon this transition, the main modification in Eq. (4.3) is the destruction of the exact degeneracy between many orbits, i.e., the reduction of γ from a value proportional to the system size to unity (or two in presence of time-reversal symmetry). However, as explained in Chapter 2, a theory based on the diagonal approximation is not capable to describe the effect of stronger disorder leading to Anderson localization. As shown in [A03], inclusion of non-trivial action correlations may remedy this flaw of the semiclassical theory, but for systems other than simple graphs this is at present beyond the state of the art.

4.2 Classical Hamiltonian ratchets

While diffusive chaotic transport is an established and well-studied scenario, it has been ignored until recently that classical transport in extended chaotic systems can also be ballistic and directed, $\overline{x} \sim t$. Flach et al. [212] investigated Hamiltonians of the form

$$H(p,x,t) = \frac{p^2}{2} + V(x) + f(t)\,x\,, \tag{4.4}$$

where $V(x)$ and $f(t)$ are periodic functions of position and time, respectively. Their numerical simulations did show a non-zero average velocity for chaotic trajectories unless specific choices of V and f lead to dynamical symmetries. In the absence of such symmetries ensembles of particles initialized with a thermal distribution start to move in one direction although the driving force averaged over space and time is zero.

Systems with this ability to generate directed motion using an unbiased periodic potential are commonly referred to as *ratchets*. Two recent reviews [213, 214] provide a comprehensive account of this subject. The investigation of ratchets was originally intended to elucidate fundamental principles of thermodynamics [215]. Later it was stimulated by the biological task of explaining the functioning of molecular motors [216] and by emerging applications such as the separation of particles [217]–[219]. Along with this process, one has tried to gain insight into the basic mechanism of ratchet transport by reducing the models under investigation as far as possible. External noise, for example, which originally served to account for the fluctuating environment of molecular motors, has been replaced by deterministic dissipative chaos [220, 221]. Seen in this context, the work of Flach et al. [212] provided the first evidence for the existence of *Hamiltonian ratchets*, where time reversal symmetry is broken by mechanisms other than friction and dissipation.

The symmetry arguments of Flach et al. make the existence of Hamiltonian ratchets plausible, but they are insufficient for a quantitative understanding of the transport. For example, they do not allow to predict direction and velocity of transport. In Refs. [222, A10] we developed a theory which closes this gap. Before we come to that we would like to explain the mechanism underlying the observed chaotic transport with an intuitive example which is again based on the Lorentz gas (Fig. 4.2a). A perpendicular magnetic field breaks the time-reversal symmetry and generates regular "skipping" trajectories which transport ballistically in one direction. Due to the particular asymmetric geometry the trajectories transporting in the opposite direction must collide with the dispersing obstacles in the channel which renders them chaotic. As a consequence one obtains a chaotic phase-space component with a non-zero mean velocity. The effect persists in a weakly disordered system provided that there exists an invariant set of transporting regular trajectories (Fig. 4.2b). We stress that the magnetic field alone is not sufficient to generate ballistic transport. In Fig. 4.2c the upper wall has obstacles as well such that the phase space is nearly completely chaotic. In this case chaotic transport is diffusive despite the absence of time-reversal symmetry.

Directed transport is obtained for an ensemble of particles prepared initially in one particular invariant set of the phase space. In this respect the billiard model is equivalent to Hamiltonian ratchets. However, in a billiard this preparation of initial conditions cannot be achieved by adjusting the mean energy (temperature) of the ensemble alone. In contrast, this is possi-

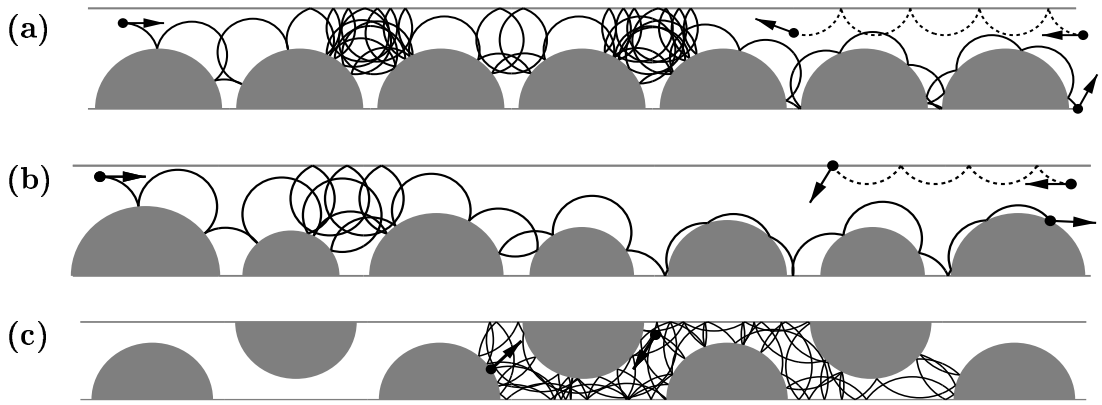

Figure 4.2: In this model, regular "skipping" trajectories (dashed lines) are induced by a magnetic field (a,b). Due to the particular geometry all such skipping orbits transport in one direction. The remaining part of phase space is mainly chaotic for the selected parameters, and therefore chaotic trajectories (full lines) compensate for the presence of the skipping orbits by an average transport in the opposite direction. This mechanism works also in the presence of disorder (b). When (almost) all regular trajectories are destroyed, however, the magnetic field alone cannot induce directed chaotic transport (c).

ble in nonequilibrium systems, with a time-dependent Hamiltonian such as Eq. (4.4). For this case a phase-space portrait is shown in Fig. 4.3. One observes a *stochastic layer* which is limited in momentum from below and above by two extended invariant tori l and u. It comprises, besides a large chaotic sea, a number of regular islands i around stable periodic orbits. These regular components play a role which is analogous to the skipping trajectories of Fig. 4.2. Note that in the model of Fig. 4.3 a thermal distribution with low temperature ($p \sim 0$) leads to initial conditions which are mainly inside the chaotic sea. Such an ensemble is tranported with some non-zero asymptotic velocity $v_{\rm ch}$.

A main result of [A10] is an expression for this chaotic velocity which is based exclusively on properties of the *regular* phase space components. $v_{\rm ch}$ depends (i) on averages of the kinetic energy $T = p^2/2$ along the extended tori l and u limiting the chaotic sea and (ii) on the areas A_i and winding

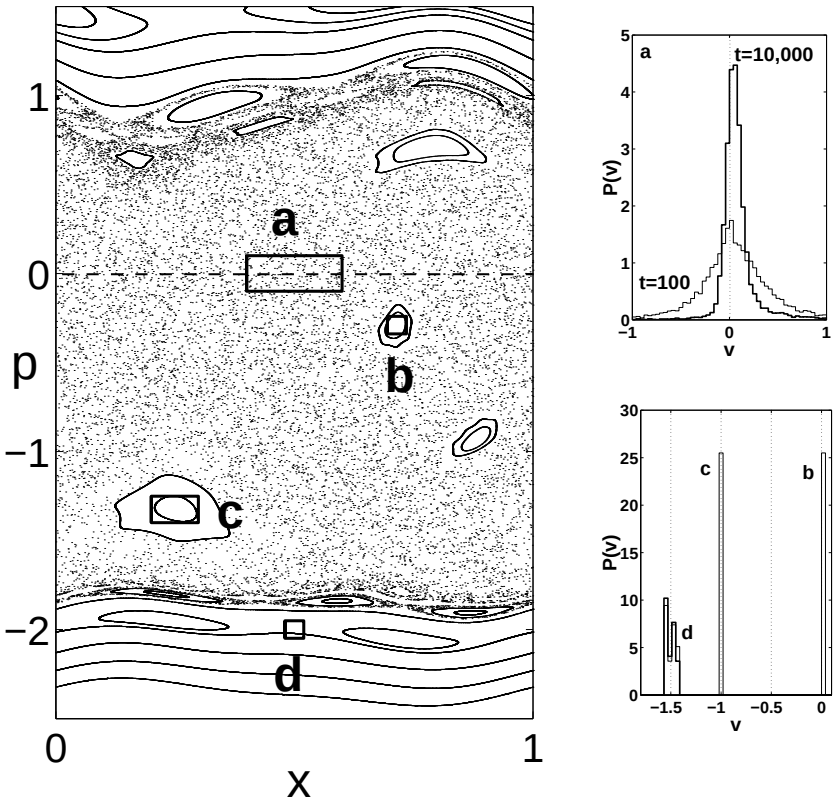

Figure 4.3: The relation between classical phase space structures and directed transport is illustrated. The left panel shows a stroboscopic Poincareé section for a spatial unit cell of a typical Hamiltonian in the form of Eq. (4.4), namely with $V(x) = [\sin(2\pi x) + 0.3\sin(4\pi x + 0.4)]/5.76$ and $f(t) = [-4.6\pi x \sin(2\pi t) - 2.76\pi x \sin(4\pi t + 0.7)]/5.76$ as in Ref. [212]. A stochastic layer consisting of a chaotic sea and embedded regular islands is limited from below and above by a region where extended regular tori dominate. Each of these different types of invariant manifolds supports directed ballistic transport. This is demonstrated by iterating a number of initial conditions chosen randomly from the rectangular regions a-d and plotting in the right panels the distribution of their velocities, averaged over 100 periods of the driving force (10,000 periods for the bold lines). For the regular initial conditions b-d 100 trajectories were used. For the chaotic sea large fluctuations in the velocity require much better statistics, but for 10,000 trajectories and long iteration time directed transport clearly leads to an asymmetric velocity distribution. According to Eq. (4.5) its mean value can be predicted by analyzing the regular regions adjacent to the chaotic sea.

numbers w_i of the embedded islands,

$$v_{\rm ch} = \frac{\langle T\rangle_u - \langle T\rangle_l - \sum_i A_i w_i}{A_{\rm layer} - \sum_i A_i}\,. \tag{4.5}$$

The derivation of this relation assumes a finite and ergodic chaotic phase-space component. Otherwise the problem is not well-defined since the existence of $v_{\rm ch}$ as the long-time limit of the transport velocity for almost all chaotic trajectories is not guaranteed and Eq. (4.5) cannot be applied. This occurs for example in systems with more than three phase-space dimensions. In this case Arnold diffusion may allow an unlimited spreading of chaotic trajectories in phase space [223, 104]. Due to this difficulty, essentially nothing is known about ratchet transport in driven Hamiltonian systems with two or more spatial dimensions.

Also in driven 1D systems the conditions for the applicability of Eq. (4.5) may be violated. Using singular potentials one can construct examples in which chaotic trajectories can absorb infinite energy from the driving force such that the stochastic layer is unlimited. It has been shown that such models can function as a type of Hamiltonian ratchet different from the one we discuss here [224].

However, in the case of quasi 1D systems with finite potentials the chaotic component is compact because for very large momenta the driving can be considered as a small perturbation and thus the regular motion of free particles is restored. In this case Eq. (4.5) applies. The essential features of such Hamiltonian ratchets can be reproduced by models for which the phase space of a unit cell is compact. A simple example is a Hamiltonian map in the form of Eq. (1.2), restricted to a cylindrical phase space. If $T(p)$ and $V(x)$ are suitably chosen one obtains a very simple phase-space structure which nevertheless displays all essential features of a Hamiltonian ratchet (Fig. 4.4). It has a single regular island transporting with velocity $v = -1$, i.e., one unit cell to the left per period of the driving. This island is embedded in a chaotic sea which shows transport in the opposite direction. In this case Eq. (4.5) takes the simple form $v_{\rm ch} = f_{\rm reg}/(1 - A_{\rm reg})$, where $f_{\rm reg}$ denotes the fraction of phase space occupied by the island. An explicit example for such a model, which we proposed in [A10] as minimal Hamiltonian ratchet, is given by

$$\begin{aligned} V(x) &= (x \bmod 1 \, - 1/2)^2/2 \\ T(p) &= |p| + 3\sin(2\pi p)/(4\pi^2)\,. \end{aligned} \tag{4.6}$$

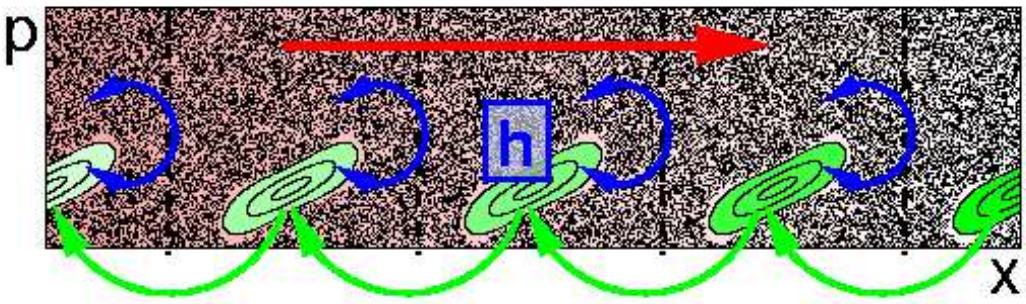

Figure 4.4: Phase-space transport in Hamiltonian ratchets. Classical transport is restricted to individual invariant manifolds, in this example a regular island transporting to the left (green) and the chaotic sea balancing this by a transport to the right (red). Quantization induces a finite resolution h in phase space which couples regular and chaotic manifolds by tunneling (blue). Therefore a wavepacket which is initially localized inside the island leaks to the chaotic sea and starts to move opposite to the island chain.

For quantized ratchets, and in particular in the presence of additional disorder, models of this type are the only way to reduce the numerical complexity to a tractable level. An additional advantage is that due to the simplicity of maps it is relatively easy to find optimal parameters which lead to very pronounced directed chaotic transport (see Fig. 1c,d of [A10]).

4.3 Semiclassical theory of quantum ratchets

Having understood the classical mechanism leading to ballistic and directed transport in Hamiltonian ratchets one may ask if this effect is present also in quantum systems, at least in the semiclassical regime. This question is not trivial although the correspondence principle guarantees that classical and quantum dynamics agree at least for some initial period. However, as one is interested in asymptotic long-time transport, non-classical processes like tunneling and localization may become important. The situation is schematically shown in Fig. 4.4 for the example of a wavepacket initially localized inside one unit cell and on one of the transporting regular islands of the system. This is the quantum analogue to an ensemble of classical trajectories (cf Fig. 4.3b). Initially, the wavepacket moves as the classical island one unit

cell to the left in one period of the driving. However, at the same time a certain fraction of the wavepacket tunnels out of the island and starts to populate the chaotic sea. Thus there is an exponentially decreasing probability of finding the quantum particle inside the island that it should have reached according to classical mechanics. A numerical confirmation of this fact is shown in Fig. 4.5b.

Actually, this figure combines data from two slightly different quantum systems which have the minimal model of Eq. (4.6) as common classical limit. We have studied them in [A10] and [A11], respectively. The difference is the effective value of Planck's constant h_{eff}, i.e., the dimensionless ratio between h and the phase-space volume of the unit cell. If it is a rational number, the quantum system is exactly periodic. For irrational h_{eff} this is not the case, despite the underlying periodic classical phase space. This can be understood intuitively if we recall that a quantum state occupies in phase space a Planck cell with area h. Thus, only for $h_{\text{eff}} = 1/q$ a single unit cell with periodic boundary conditions can be exactly tiled by $q \in \mathbb{N}$ Planck cells. For a general rational $h_{\text{eff}} = p/q$ this is possible for the union of p unit cells, while for irrational h_{eff} only the infinite system allows for a proper quantization.

As changing a rational into an irrational h_{eff} requires only a small difference, the rate for tunneling out of the island is hardly affected and the probability of being inside the classically expected unit cell is essentially the same for the two models (Fig. 4.5b and inset of 4.5a). However, the fate of the part of the wavepacket that has reached the chaotic sea is entirely different (Fig. 4.5a). In the exactly periodic model most of the probability tunnels back into the transporting island, albeit not in the classical unit cell but in those lagging slightly behind. Effectively the major part of the wavepacket remains thus in the island chain and the asymptotic quantum transport velocity approaches the classical one in the semiclassical limit $h \to 0$ (see also Fig. 2 of [A10]). In contrast, for the aperiodic model an equilibration between island chain and chaotic sea takes place such that the transport velocity asymptotically vanishes.

It is very hard to understand this difference from a purely dynamical point of view, as details of the interference between the regular and the chaotic parts of the packet are important. A much clearer picture of the long-time behaviour is obtained by studying the eigenfunctions in the periodic and the aperiodic ratchet models.

For the periodic case there is a band spectrum (Fig. 4.6a) and the asymp-

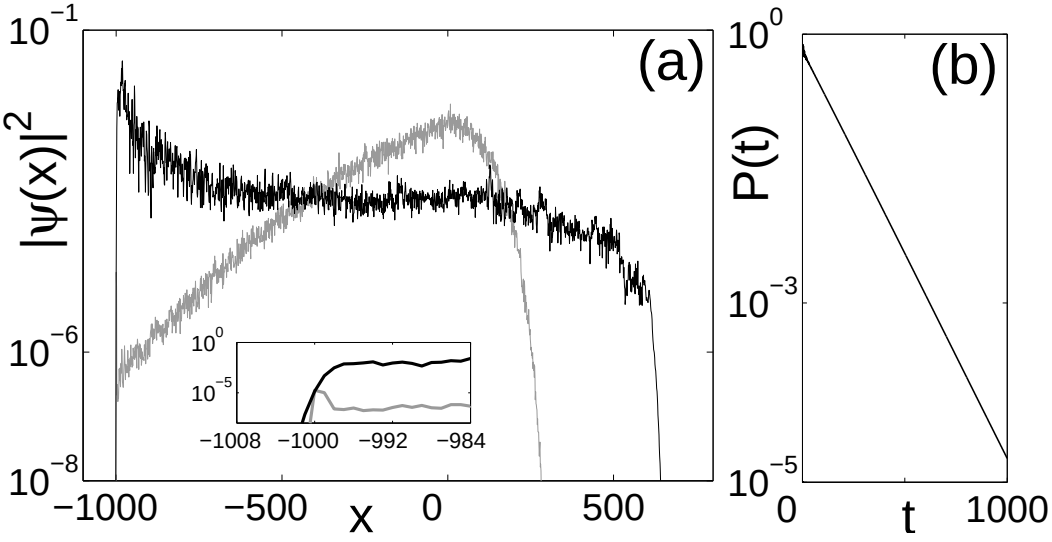

Figure 4.5: (a) Black line: Wave packet prepared in the regular island of the unit cell $x = 0$ and propagated to time $t = 1000$ in the minimal ratchet model Eq. (4.6) with $h^{-1} = 16$. The classical probability would be restricted to the unit cell $x = -1000$, while the quantum wavepacket has tunneled out of this "classical" unit cell and starts spreading. A large peak remains, however, slightly behind the classically expected position. Gray line: Same for irrational $h^{-1} = 16 + \sigma$ ($\sigma = (\sqrt{5} - 1)/2$ is the golden mean). In this case the Floquet operator has no spatial periodicity. The part of the wave packet outside the classical unit cell localizes and develops an asymmetric envelope with approximately exponential tails. Inset: The probability remaining inside the classical unit cell $x = -1000$ is the same for rational and irrational h but the distribution of the probability in the neighboring cells is drastically different (note the logarithmic scale). (b) Due to dynamical tunneling the quantum probability in the classical unit cell decays exponentially as a function of time. With respect to this decay the periodic model with $h^{-1} = 16$ is almost indistinguishable from the aperiodic model with irrational $h^{-1} = 16 + \sigma$.

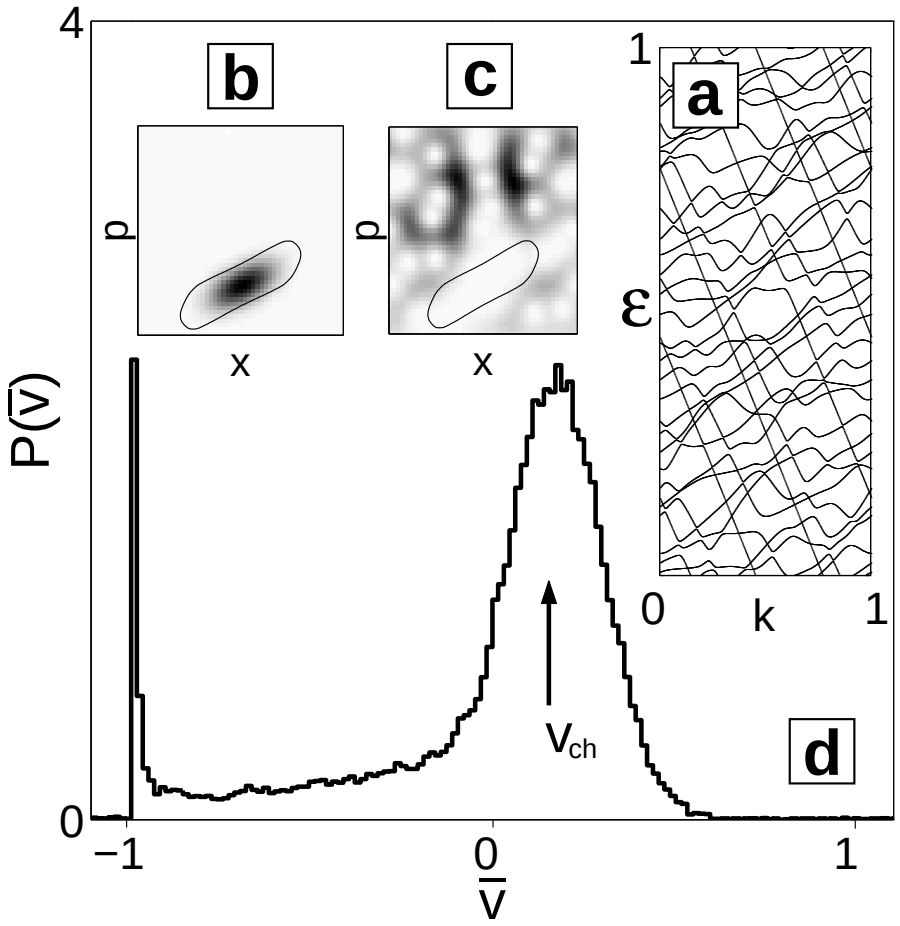

Figure 4.6: (a) Quasienergy band spectrum of the minimal ratchet model Eq. (4.6) at $h^{-1} = 32$. Regular bands appear as approximately straight lines with negative slope. (b) The Husimi representation of the Floquet eigenstates corresponding to these points in the spectrum are concentrated inside the regular island. (c) Most other eigenfunctions spread over the entire chaotic sea but avoid the regular island. The corresponding bands have strongly fluctuating slopes. (d) Distribution of band slopes (velocity expectation values) at $h^{-1} = 128$. The sharp peak at $v = -1$ corresponds to the regular bands, the broader peak to the chaotic bands. The velocity of the classically chaotic transport is marked by an arrow.

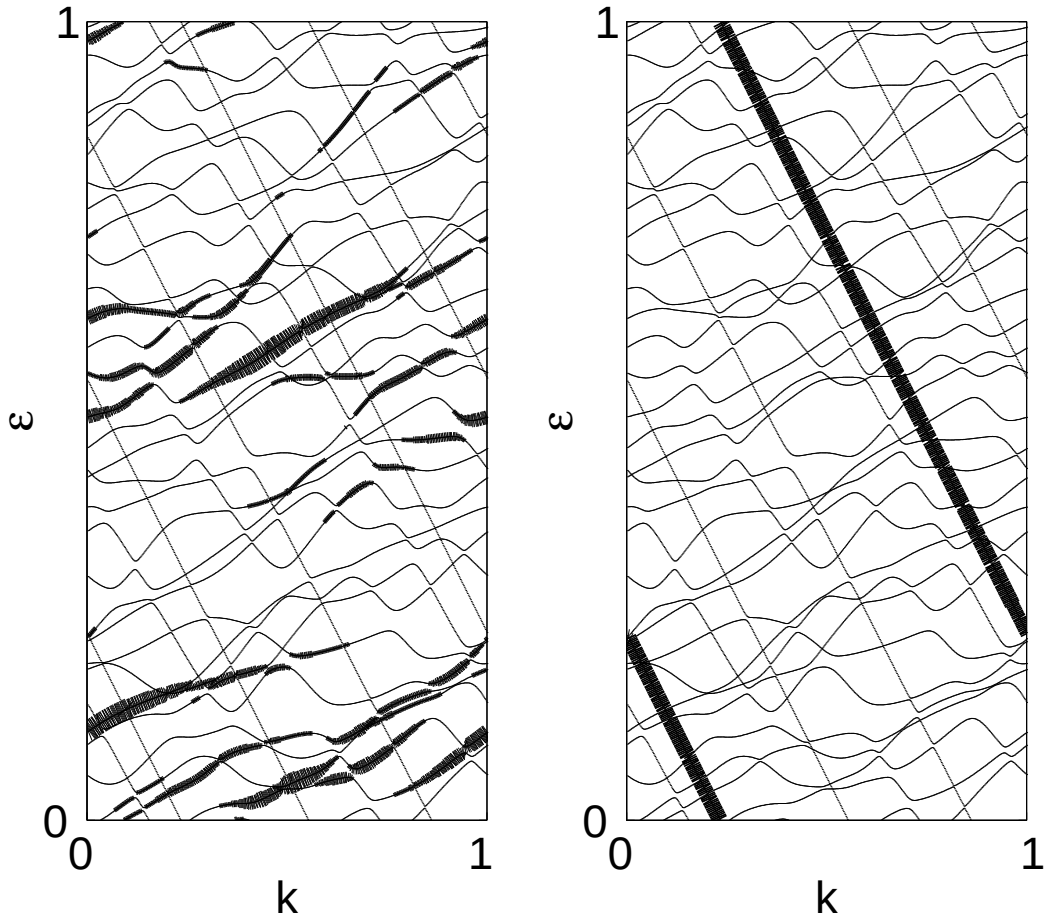

Figure 4.7: Quasienergy band spectrum of the minimal ratchet model at $h^{-1} = 32$. The linewidth encodes the overlap $|\langle\phi_{\alpha,k}|\psi\rangle|^2$ of the corresponding Floquet state $|\phi_{\alpha,k}\rangle$ with an initial wavepacket $|\psi\rangle$. In (a) this wavepacket is a coherent state located in the chaotic part of the phase space of a single unit cell, in (b) it is concentrated on a torus inside the regular island.

totic transport velocity of a state is simply given by the band slope. The eigenstates are spatially extended, but they are localized in the phase space of a unit cell on one of the classically invariant manifolds, i.e., there are regular and chaotic eigenstates (Fig. 4.6b,c). As explained in Chapter 1, this is expected from the semiclassical eigenfunction hypothesis which does apply here since due to the periodicity each unit cell represents effectively a finite system. The corresponding band slopes are close to the classical transport velocity v_{reg} of the island for the regular states and distributed around the chaotic velocity v_{ch} for the chaotic ones (Fig. 4.6d). With the help of a quantum sum rule analogous to Eq. (4.5) we have formulated this fact more quantitatively [A10]. Coming back to the asymptotic transport of a wavepacket, one has a superposition of eigenstates. For a wavepacket localized initially inside one unit cell and on the regular/chaotic subset of phase space this superposition will include regular/chaotic states from the whole Brillouin zone (Fig. 4.7) and thus the asymptotic transport will be close to an average over the respective band slopes. Using these arguments it becomes clear that the ratchet transport persists in the exactly periodic quantum model despite the presence of tunneling. A more detailed analysis of the band spectrum can also explain the conspicuous shape of the evolving wavepacket shown in Fig. 4.5, with a peak that is slightly behind the classical unit cell [211].

In the aperiodic case the localization properties of the eigenstates are exactly opposite to the periodic one: they are spatially localized but do not show any localization with respect to the classical phase-space structures. We have developed a theory which establishes that this behaviour is retained in the semiclassical limit [A11]. Thus, Hamiltonian ratchets with disorder are the first example of a system to which the semiclassical eigenfunction hypothesis does *not* apply. All eigenstates are of a novel "amphibious" type and spread equally over the chaotic sea and the regular islands. Another interesting property of these amphibious states is their giant localization length which grows exponentially with decreasing h_{eff}. Transport of wavepackets must cease finally due to localization, but in the semiclassical limit it persists to exponentially long times. How precisely this transport is encoded in the eigenstates is unknown at present, and the detailed nature of the amphibious states remains a rich field for further investigation.

Summary and outlook

We have presented a number of selected results concerning the quantum properties of nonintegrable systems. Hopefully it has become clear that interesting and nontrivial problems exist in this field already in a simplified situation in which a single-particle description is valid and important physical effects such as decoherence and dissipation are neglected. The theoretical investigation of such an idealized setting is justified and motivated by growing experimental capabilities to realize very "clean" systems, in which highly excited states retain quantum coherence over a very long time. Such systems provide applications for the semiclassical theory of spectra and eigenstates in the presence of classical chaos to which we have contributed.

After more than 30 years of intense research quantum chaos has come of age to some extent. In particular the properties of systems with an unstructured and completely chaotic phase space are well understood thanks to the success of random-matrix theory. Recent progress in semiclassical methods warrants the hope that many of the predictions of RMT can soon be derived directly from the underlying chaotic dynamics, with precise statements on their range of validity.

Therefore, RMT plays nowadays mainly the role of a benchmark, and of primary physical interest are the deviations from it. We have explained that there exist *universal* quantum manifestations of the system-specific classical dynamics, which can be met in all quantized chaotic systems irrespective of the concrete physical realization. Because of this universality, valuable insight can be gained from minimal models such as billiards, Hamiltonian maps and quantum graphs as long as it is not possible to formulate a completely general semiclassical theory.

Indeed this ultimate goal is still far from being realized, at least in systems in which the classical phase space is mixed or structured in some other way, and this leaves plenty room for future work.

Bibliography

[1] M. C. Gutzwiller. *Chaos in Classical and Quantum Mechanics.* Springer, New York, 1990.

[2] F. Haake. *Quantum Signatures of Chaos.* Springer, Berlin, 2000.

[3] H.-J. Stöckmann. *Quantum chaos: an introduction.* Cambridge Univ. Press, Cambridge, 1999.

[4] M. J. Giannoni, A. Voros, and J. Zinn-Justin, editors. *Chaos and quantum physics.* Session LII of the Les Houches Summer School of Theoretical Physics, 1989. North-Holland, Amsterdam, 1991.

[5] G. Casati, I. Guarneri, and U. Smilansky, editors. *Caos quantico*, volume CXIX of *the Proceedings of the International School of Physics "Enrico Fermi".* North-Holland, Amsterdam, 1993.

[6] G. Casati and B. V. Chirikov, editors. *Quantum Chaos.* Cambridge University Press, Cambridge, 1995.

[7] I. V. Lerner, J. P. Keating, and D. E. Khmelnitskii, editors. *Proceedings of a NATO Advanced Study Institute on Supersymmetry and Trace Formulae: Chaos and Disorder, Cambridge 1997*, volume B370 of *the NATO ASI Series.* Kluwer Academic/Plenum, New York, 1998.

[8] G. Casati, I. Guarneri, and U. Smilansky, editors. *New Directions in Quantum Chaos*, volume CXLIII of *the Proceedings of the International School of Physics "Enrico Fermi".* North-Holland, Amsterdam, 2000.

[9] K. F. Berggren, P. Omling, and S. Aberg, editors. *Quantum Chaos Y2K - Proceedings of the Nobel Symposium 116 Backaskog Castle, Sweden, 2000*, volume T90 of *Physica Scripta.* 2001.

[10] M. Berry. Quantum chaology, not quantum chaos. *Physica Scripta*, 40:335, 1989.

[11] V. Zelevinsky et al. The nuclear shell model as a testing ground for many-body quantum chaos. *Phys. Rep.*, 276:85, 1996.

[12] M. Brack, S. M. Reimann, and M. Sieber. Semiclassical interpretation of the mass asymmetry in nuclear fission. *Phys. Rev. Lett.*, 79:1817, 1997.

[13] V. Zelevinsky. Many-body aspects of quantum chaos. *Int. J. Mod. Phys. B*, 13:569, 1999.

[14] M. Brack, M. Sieber, and S. M. Reimann. Wavefunction localization and its semiclassical description in a 3-dimensional system with mixed classical dynamics. *Phys. Scr.*, T90:146, 2001.

[15] S. J. Wang and Q. L. Jie. General features of quantum chaos and its relevance to nuclear physics. *Phys. Rev. C*, 6301:450, 2001.

[16] V. G. Zelevinsky. Nuclear physics and ideas of quantum chaos. *Phys. At. Nuc.*, 65:1188, 2002.

[17] R. V. Jensen. Chaos in atomic physics. *Atomic Physics*, 10:319, 1987.

[18] R. V. Jensen. Quantum chaos. *Nature*, 355:311, 1992.

[19] F. L. Moore et al. Atom optics realization of the quantum delta-kicked rotor. *Phys. Rev. Lett.*, 75:4598, 1995.

[20] M. G. Raizen et al. Experimental study of quantum chaos with cold atoms. In G. Casati, I. Guarneri, and U. Smilansky, editors, *New Directions in Quantum Chaos*, volume CXLIII of *the Proceedings of the International School of Physics "Enrico Fermi"*, page 299. North-Holland, Amsterdam, 2000.

[21] V. V. Flambaum et al. Quantum chaos in many-body systems: what can we learn from the ce atom? *Physica D*, 131:205, 1999.

[22] V. Milner et al. Optical billiards for atoms. *Phys. Rev. Lett.*, 86:1514, 2001.

[23] N. Friedman et al. Observation of chaotic and regular dynamics in atom-optics billiards. *Phys. Rev. Lett.*, 86:1518, 2001.

[24] A. Kaplan et al. Observation of islands of stability in soft wall atom-optics billiards. *Phys. Rev. Lett.*, 87:274101, 2001.

[25] W. P. Reinhardt and S. B. McKinney. Dynamical and wave chaos in the Bose-Einstein condensate. *Phys. Scr.*, T90:202, 2001.

[26] M. A. Porter and R. L. Liboff. A Galerkin approach to electronic near-degeneracies in molecular systems. *Physica D*, 167:218, 2002.

[27] C. M. Marcus et al. Conductance fluctuations and chaotic scattering in ballistic microstructures. *Phys. Rev. Lett.*, 69:506, 1992.

[28] J. P. Bird. Recent experimental studies of electron transport in open quantum dots. *J. Phys.-Cond. Mat.*, 11:R413, 1999.

[29] Y. Alhassid. The statistical theory of quantum dots. *Rev. Mod. Phys.*, 72:895, 2000.

[30] A. M. Chang. Quantum chaos in GaAs/AlxGa1-xAs microstructures. *Phys. Scr.*, T90:16, 2001.

[31] A. S. Sachrajda. Quantum chaos and transport phenomena in quantum dots. *Phys. Scr.*, T90:34, 2001.

[32] Y. Alhassid. Chaos and interactions in quantum dots. *Phys. Scr.*, T90:80, 2001.

[33] E. Doron, U. Smilansky, and A. Frenkel. Experimental demonstration of chaotic scattering of microwaves. *Phys. Rev. Lett.*, 65:3072, 1990.

[34] H.-J. Stöckmann and J. Stein. "Quantum" chaos in billiards studied by microwave absorption. *Phys. Rev. Lett.*, 64:2215, 1990.

[35] S. Sridhar. Experimental-observation of scarred eigenfunctions of chaotic microwave cavities. *Phys. Rev. Lett.*, 67:785, 1991.

[36] H. D. Graf et al. Distribution of eigenmodes in a superconducting stadium billiard with chaotic dynamics. *Phys. Rev. Lett.*, 69:1296, 1992.

[37] W. T. T. Lu et al. Quantum correlations and classical resonances in an open chaotic system. *Phys. Scr.*, T90:238, 2001.

[38] A. Richter. Wave dynamical chaos: An experimental approach in billiards. *Phys. Scr.*, T90:212, 2001.

[39] H. J. Stöckmann. Why do an experiment, if theory is exact, and any experiment can at best approximate theory? *Phys. Scr.*, T90:246, 2001.

[40] J. U. Nöckel and A. D. Stone. Ray and wave chaos in asymmetric resonant optical cavities. *Nature*, 385:45, 1997.

[41] C. Gmachl et al. High-power directional emission from microlasers with chaotic resonators. *Science*, 280:1556, 1998.

[42] A. D. Stone. Wave-chaotic optical resonators and lasers. *Phys. Scr.*, T90:248, 2001.

[43] C. Ellegaard et al. Symmetry breaking and spectral statistics of acoustic resonances in quartz blocks. *Phys. Rev. Lett.*, 77:4918, 1996.

[44] P. Bertelsen et al. Measurement of parametric correlations in spectra of resonating quartz blocks. *Phys. Rev. Lett.*, 83:2171, 1999.

[45] C. Ellegaard, K. Schaadt, and P. Bertelsen. Acoustic chaos. *Phys. Scr.*, T90:223, 2001.

[46] M. Fink. Chaos and time-reversed acoustics. *Phys. Scr.*, T90:268, 2001.

[47] K. Schaadt, G. Simon, and C. Ellegaard. Ultrasound resonances in a rectangular plate described by random matrices. *Phys. Scr.*, T90:231, 2001.

[48] A. Bulgac and P. Magierski. Neutron stars and quantum billiards. *Phys. Scr.*, T90:150, 2001.

[49] R. Graham. Chaos and quantum chaos in cosmological models. *Chaos Solitons & Fractals*, 5:1103, 1995.

[50] O. Bohigas, M. J. Giannoni, and C. Schmit. Characterization of chaotic quantum spectra and universality of level fluctuation laws. *Phys. Rev. Lett.*, 52:1, 1984.

[51] E. P. Wigner. Random matrices in physics. *SIAM Rev.*, 9:1, 1967.

[52] R. Blümel et al. Dynamical localization in the microwave interaction of Rydberg atoms: The influence of noise. *Phys. Rev. A*, 44:4521, 1991.

[53] M. L. Mehta. *Random Matrices.* Academic Press, New York, 1991.

[54] J. J. M. Verbaarschot, H. A. Weidenmüller, and M. R. Zirnbauer. Grassmann integration in stochastic quantum physics - the case of compound nucleus scattering. *Phys. Rep.*, 129:367, 1985.

[55] K. Efetov. Supersymmetry in quantum chaos and mesoscopic physics. *Physica D*, 83:151, 1995.

[56] K. Efetov. *Supersymmetry in disorder and chaos.* Cambridge Univ. Press, Cambridge, 1997.

[57] C. W. J. Beenakker. Random-matrix theory of quantum transport. *Rev. Mod. Phys.*, 69:731, 1997.

[58] T. Guhr, A. Müller-Groeling, and H. A. Weidenmüller. Random-matrix theories in quantum physics: Common concepts. *Phys. Rep.*, 299:190, 1998.

[59] M. C. Gutzwiller. Energy spectrum according to classical mechanics. *J. Math. Phys.*, 11:1791, 1970.

[60] M. C. Gutzwiller. Periodic orbits and classical quantization conditions. *J. Math. Phys.*, 12:343, 1971.

[61] M. V. Berry. Semiclassical theory of spectral rigidity. *Proc. R. Soc. Lond. A*, 400:229, 1985.

[62] I. C. Percival. Regular and irregular spectra. *J. Phys. B*, 6:L229, 1973.

[63] M. V. Berry. Regular and irregular semiclassical wavefunctions. *J. Phys. A*, 10:2083, 1977.

[64] M. V. Berry and M. Robnik. Semiclassical level spacings when regular and chaotic orbits coexist. *J. Phys. A*, 17:2413, 1984.

[65] R. Ketzmerick, L. Hufnagel, F. Steinbach, and M. Weiss. New class of eigenstates in generic Hamiltonian systems. *Phys. Rev. Lett.*, 85:1214, 2000.

[66] L. Hufnagel, R. Ketzmerick, and M. Weiss. Conductance fluctuations of generic billiards: Fractal or isolated? *Europhys. Lett.*, 54:703, 2001.

[67] V. A. Podolskiy and E. E. Narimanov. Universal level-spacing distribution in quantum systems. Preprint nlin.CD/0310034, 2003.

[68] A. Katok and J. Strelcyn. *Invariant manifolds, entropy and billiards: smooth maps with singularities*, volume 1222 of *Lecture notes in mathematics*. Springer, Berlin, 1986.

[69] O. Biham and M. Kvale. Unstable periodic orbits in the stadium billiard. *Phys. Rev. A*, 46:6334, 1992.

[70] L. A. Bunimovich. Variational principle for periodic trajectories of hyperbolic billiards. *Chaos*, 5:349, 1995.

[71] H. Schanz. On finding the periodic orbits of the Sinai billiard. In J. A. Freund, editor, *Dynamik, Evolution, Strukturen*. Verlag Dr. Köster, Berlin, 1996.

[72] A. Bäcker and H. R. Dullin. Symbolic dynamics and periodic orbits for the cardioid billiard. *J. Phys. A*, 30:1991, 1997.

[73] Ya. G. Sinai. Dynamical systems with elastic reflections. *Russian Mathematical Survey*, 25:137, 1970.

[74] L. A. Bunimovich. *Funct. Anal. Appl.*, 8:254, 1974.

[75] M. Wojtkowski. Principles for the design of billiards with nonvanishing Lyapunov exponents. *Comm. Math. Phys.*, 105:391, 1986.

[76] D. Szasz. On the K-property of some planar hyperbolic billiards. *Comm. Math. Phys.*, 145:595, 1992.

[77] R. Markarian. New ergodic billiards - exact results. *Nonlinearity*, 6:819, 1993.

[78] D. Biswas and S. R. Jain. Quantum description of a pseudointegrable system - the pi-3-rhombus billiard. *Phys. Rev. A*, 42:3170, 1990.

[79] A. Shudo et al. Statistical properties of spectra of pseudointegrable systems. *Phys. Rev. E*, 49:3748, 1994.

[80] T. Gorin. Generic spectral properties of right triangle billiards. *J. Phys. A*, 34:8281, 2001.

[81] A. Bäcker, R. Schubert, and P. Stifter. On the number of bouncing ball modes in billiards. *J. Phys. A*, 30:6783, 1997.

[82] A. Bäcker et al. Isolated resonances in conductance fluctuations in ballistic billiards. *Physica E*, 18:149, 2003.

[83] E. Doron and S. D. Frischat. Semiclassical description of tunneling in mixed systems - case of the annular billiard. *Phys. Rev. Lett.*, 75:3661, 1995.

[84] C. Dembowski et al. First experimental evidence for chaos-assisted tunneling in a microwave annular billiard. *Phys. Rev. Lett.*, 84:867, 2000.

[85] O. Brodier, P. Schlagheck, and D. Ullmo. Resonance-assisted tunneling. *Ann. Phys. (N.Y.)*, 300:88, 2002.

[86] M. Hentschel and K. Richter. Quantum chaos in optical systems: The annular billiard. *Phys. Rev. E*, 66:149, 2002.

[87] L. A. Bunimovich. Mushrooms and other billiards with divided phase space. *Chaos*, 11:802, 2001.

[88] B. Gutkin. Can billiard eigenstates be approximated by superpositions of plane waves? *J. Phys. A*, 36:8603, 2003.

[89] D. Cohen, N. Lepore, and E. J. Heller. Consolidating boundary methods for finding the eigenstates of billiards. Preprint nlin.CD/0108014, 2001.

[90] A. Bäcker. Numerical aspects of eigenvalue and eigenfunction computations for chaotic quantum systems. Preprint nlin.CD/0204061, 2002.

[91] E. Doron and U. Smilansky. Semiclassical quantization of chaotic billiards: A scattering theory approach. *Nonlinearity*, 5:1055, 1992.

[92] U. Smilansky. Semiclassical quantization of chaotic billiards – A scattering approach. In E. Akkermans, G. Montambaux, and J. L. Pichard, editors, *Mesoscopic Quantum Physics*, Les Houches Summer School Sessions LXI, Amsterdam, 1996. North-Holland.

[93] E. Vergini and M. Saraceno. Calculation by scaling of highly excited-states of billiards. *Phys. Rev. E*, 52:2204, 1995.

[94] G. Vattay, A. Wirzba, and P. E. Rosenqvist. Periodic orbit theory of diffraction. *Phys. Rev. Lett.*, 73:2304, 1994.

[95] N. Pavloff and C. Schmit. Diffractive orbits in quantum billiards. *Phys. Rev. Lett.*, 75:61, 1995.

[96] H. Primack et al. Penumbra diffraction in the quantization of dispersing billiards. *Phys. Rev. Lett.*, 76:1615, 1996.

[97] M. Sieber, N. Pavloff, and C. Schmit. Uniform approximation for diffractive contributions to the trace formula in billiard systems. *Phys. Rev. E*, 55:2279, 1997.

[98] M. V. Berry. Quantizing a classically ergodic system: The Sinai billiard and the KKR method. *Ann. Phys.*, 131:163, 1981.

[99] M. Sieber et al. Nongeneric spectral statistics in the quantized stadium billiard. *J. Phys. A*, 26:6217, 1993.

[100] E. J. Heller, M. F. Crommie, C. P. Lutz, and D. M. Eigler. Scattering and absorption of surface electron waves in quantum corrals. *Nature*, 369:464, 1994.

[101] H. C. Manoharan, C. P. Lutz, and D. M. Eigler. Quantum mirages formed by coherent projection of electronic structure. *Nature*, 403:512, 2000.

[102] E. Arcos et al. Vibrating soap films: An analog for quantum chaos on billiards. Preprint chao-dyn/9903002, 1999.

[103] H. Alt et al. Wave dynamical chaos in a superconducting three-dimensional Sinai billiard. *Phys. Rev. Lett.*, 79:1026, 1997.

[104] B. V. Chirikov. Universal instability of many-dimensional oscillator systems. *Phys. Rep.*, 52:263, 1979.

[105] F. M. Izrailev. Simple models of quantum chaos - spectrum and eigenfunctions. *Phys. Rep.*, 196:299, 1990.

[106] T. Kottos and U. Smilansky. Periodic orbit theory and spectral statistics for quantum graphs. *Ann. Phys.*, 274:76, 1999.

[107] R. Klesse and M. Metzler. Modeling disordered quantum systems with dynamical networks. *Int. J. Mod. Phys. C*, 10:577, 1999.

[108] P. Kuchment. Graph models for waves in thin structures. *Waves in Random Media*, 12:R1, 2002.

[109] *Proceedings of the 33rd ACM Annual Symposium on the Theory of Computing*, New York, 2001. ACM Press.

[110] T. Kottos and U. Smilansky. Quantum chaos on graphs. *Phys. Rev. Lett.*, 79:4794, 1997.

[111] T. Kottos and U. Smilansky. Chaotic scattering on graphs. *Phys. Rev. Lett.*, 85:968, 2000.

[112] F. Barra and P. Gaspard. Transport and dynamics on open quantum graphs. *Phys. Rev. E*, 65:101, 2002.

[113] T. Kottos and U. Smilansky. Quantum graphs: a simple model for chaotic scattering. *J. Phys. A*, 36:3501, 2003.

[114] T. Kottos and H. Schanz. Statistical properties of resonance widths for open quantum graphs. *Waves Random Media*, 14:S91, 2004.

[115] M. Puhlmann. Quantengraphen als Modell für offene Quantensysteme. Diploma thesis, University of Göttingen, 2003.

[116] M. F. Otto. *Dynamics and eigenfunctions of Hamiltonian ratchets.* PhD thesis, University of Göttingen, 2002.

[117] F. Barra and T. Gilbert. Algebraic decay in hierarchical graphs. *J. Stat. Phys.*, 109:777, 2002.

[118] M. Puhlmann, H. Schanz, T. Kottos, and T. Geisel. Quantum dynamics of open chaotic systems: A semiclassical approach. in preparation, 2004.

[119] G. Berkolaiko. *Quantum Star Graphs and Related Systems*. PhD thesis, University of Bristol, UK, 2000.

[120] G. Berkolaiko and J. P. Keating. Two-point spectral correlations for star graphs. *J. Phys. A*, 32:7827, 1999.

[121] G. Tanner. Spectral statistics for unitary transfer matrices of binary graphs. *J. Phys. A*, 33:3567, 2000.

[122] H. Schanz and U. Smilansky. Combinatorial identities from the spectral theory of quantum graphs. *The Electronic Journal of Combinatorics*, 8:R16, 2001.

[123] G. Berkolaiko, E. B. Bogomolny, and J. P. Keating. Star graphs and Šeba billiards. *J. Phys. A*, 34:335, 2001.

[124] G. Tanner. Unitary-stochastic matrix ensembles and spectral statistics. *J. Phys. A*, 34:8485, 2001.

[125] P. Pakonski, K. Zyczkowski, and M. Kus. Classical 1d maps, quantum graphs and ensembles of unitary matrices. *J. Phys. A*, 34:9303, 2001.

[126] G. Tanner. The autocorrelation function for spectral determinants of quantum graphs. *J. Phys. A*, 35:5985, 2002.

[127] J. Bolte and J. Harrison. Spectral statistics for the Dirac operator on graphs. *J. Phys. A*, 36:2747, 2003.

[128] J. Bolte and J. Harrison. The spin contribution to the form factor of quantum graphs. *J. Phys. A*, 36:L433, 2003.

[129] T. Nagao and K. Saito. Form factor of a quantum graph in a weak magnetic field. *Phys. Lett.*, 311:353, 2003.

[130] S. Gnutzmann et al. Universal spectral statistics of Andreev billiards: Semiclassical approach. *Phys. Rev. E*, 67:046225, 2003.

[131] S. Gnutzmann and B. Seif. Universal spectral statistics in Wigner-dyson, chiral and Andreev star graphs i: construction and numerical results. Preprint nlin.CD/0309049, 2003.

[132] L. Kaplan. Eigenstate structure in graphs and disordered lattices. *Phys. Rev. E*, 64:036225, 2001.

[133] J. P. Keating, J. Marklof, and B. Winn. Value distribution of the eigenfunctions and spectral determinants of quantum star graphs. Preprint math-ph/0210060, 2002.

[134] S. Gnutzmann, U. Smilansky, and J. Weber. Nodal counting on quantum graphs. *Waves Random Media*, 14:S61, 2004.

[135] G. Berkolaiko, J. P. Keating, and B. Winn. No quantum ergodicity for star graphs. Preprint math-ph/0308005.

[136] G. Berkolaiko, J. P. Keating, and B. Winn. Intermediate wave function statistics. *Phys. Rev. Lett.*, 91:134103, 2003.

[137] B. Gutkin and U. Smilansky. Can one hear the shape of a graph? *J. Phys. A*, 34:6061, 2001.

[138] R. Blümel and Y. Dabaghian. Combinatorial identities for binary necklaces from exact ray-splitting trace formulas. *J. Math. Phys.*, 42:5832, 2001.

[139] Y. Dabaghian, R. V. Jensen, and R. Blümel. One-dimensional quantum chaos: Explicitly solvable cases. *JETP Lett.*, 74:235, 2001.

[140] R. Blümel, Y. Dabaghian, and R. V. Jensen. Explicitly solvable cases of one-dimensional quantum chaos. *Phys. Rev. Lett.*, 88:044101, 2002.

[141] Y. Dabaghian, R. V. Jensen, and R. Blümel. Spectra of regular quantum graphs. *JETP*, 94:1201, 2002.

[142] R. Blümel, Y. Dabaghian, and R. V. Jensen. Exact, convergent periodic-orbit expansions of individual energy eigenvalues of regular quantum graphs. *Phys. Rev. E*, 65:1201, 2002.

[143] Z. Q. Zhang and P. Sheng. Wave localization in random networks. *Phys. Rev. B*, 49:83, 1994.

[144] Z. Q. Zhang et al. Observation of localized electromagnetic waves in three- dimensional networks of waveguides. *Phys. Rev. Lett.*, 81:5540, 1998.

[145] N. Sondergaard and G. Tanner. Wave chaos in the elastic disk. *Phys. Rev. E*, 66:066211, 2002.

[146] A. Einstein. *Verh. Dtsch. Phys. Ges.*, 19:82, 1917.

[147] R. Feynman. Space-time approach to non-relativistic quantum mechanics. *Rev. Mod. Phys.*, 20:367, 1948.

[148] J. H. Van Vleck. *Proc. Nat. Ac. Sc. USA*, 14:178, 1928.

[149] M. V. Berry and J. P. Keating. A rule for quantizing chaos? *J. Phys. A*, 23:4839, 1990.

[150] E. B. Bogomolny. Semiclassical quantization of multidimensional systems. *Nonlinearity*, 5:805, 1992.

[151] J. P. Keating. Periodic orbit resummation and the quantization of chaos. *Proc. R. Soc. Lond. A*, 436:99, 1992.

[152] B. Georgeot and R. E. Prange. Exact and quasi-classical fredholm solutions of quantum billiards. *Phys. Rev. Lett.*, 74:2851, 1995.

[153] W. H. Miller. Classical-limit quantum mechanics and the theory of molecular collisions. *Adv. Chem. Phys.*, 25:69, 1974.

[154] C. Jung. Poincaré map for scattering states. *J. Phys. A: Math. Gen.*, 19:1345, 1986.

[155] U. Smilansky. The classical and quantum theory of chaotic scattering. In M. J. Giannoni, A. Voros, and J. Zinn-Justin, editors, *Les Houches 1989 Session LII, Chaos and Quantum Physics*, page 371. North-Holland, Amsterdam, 1991.

[156] R. A. Jalabert, H. U. Baranger, and A. D. Stone. Conductance fluctuations in the ballistic regime: A probe of quantum chaos? *Phys. Rev. Lett.*, 65:2442, 1990.

[157] R. A. Jalabert. The semiclassical tool in mesoscopic physics. In G. Casati, I. Guarneri, and U. Smilansky, editors, *New Directions in Quantum Chaos*, volume CXLIII of *the Proceedings of the International School of Physics "Enrico Fermi"*, page 145. North-Holland, Amsterdam, 2000.

[158] T. Prosen. General quantum surface-of-section method. *J. Phys. A*, 28:4133, 1995.

[159] E. J. Heller. Time-dependent variational approach to semiclassical dynamics. *J. Chem. Phys.*, 64:63, 1976.

[160] E. J. Heller. Wave packet dynamics and quantum chaology. In M. J. Giannoni, A. Voros, and J. Zinn-Justin, editors, *Chaos and Quantum Physics*, Les Houches Summer School Sessions LII, Amsterdam, 1991. North-Holland.

[161] O. Agam, B. L. Altshuler, and A. V. Andreev. Spectral statistics - from disordered to chaotic systems. *Phys. Rev. Lett.*, 75:4389, 1995.

[162] A. V. Andreev et al. Quantum chaos, irreversible classical dynamics, and random matrix theory. *Phys. Rev. Lett.*, 76:3947, 1996.

[163] A. Altland and M. R. Zirnbauer. Field theory of the quantum kicked rotor. *Phys. Rev. Lett.*, 77:4536, 1996.

[164] J. H. Hannay and A. M. Ozorio de Almeida. Periodic orbits and a correlation function for the semiclassical density of states. *J. Phys. A*, 17:3429, 1984.

[165] L. P. Kadanoff and C. Tang. Escape from strange repellers. *Proc. Nat. Ac. Sc. USA*, 81:1276, 1984.

[166] N. Argaman, Y. Imry, and U. Smilansky. Semiclassical analysis of spectral correlations in mesoscopic systems. *Phys. Rev. B*, 47:4440, 1993.

[167] N. Argaman et al. Correlations in the actions of periodic-orbits derived from quantum chaos. *Phys. Rev. Lett.*, 71:4326, 1993.

[168] D. Cohen, H. Primack, and U. Smilansky. Quantal-classical duality and the semiclassical trace formula. *Ann. Phys.*, 264:108, 1998.

[169] U. Smilansky and B. Verdene. Action correlations and random matrix theory. *J. Phys. A*, 36:3525, 2003.

[170] M. V. Berry and J. P. Keating. The Riemann zeros and eigenvalue asymptotics. *SIAM Rev.*, 41:236, 1999.

[171] T. Kottos and H. Schanz. Quantum graphs: a model for quantum chaos. *Physica E*, 9:523, 2001.

[172] M. Sieber and K. Richter. Correlations between periodic orbits and their role in spectral statistics. *Phys. Scr.*, T90:128, 2001.

[173] M. Sieber. Leading off-diagonal approximation for the spectral form factor for uniformly hyperbolic systems. *J. Phys. A*, 35:613, 2002.

[174] K. Richter and M. Sieber. *Phys. Rev. Lett.*, 89:206801, 2002.

[175] P. A. Braun, F. Haake, and S. Heusler. Action correlation of orbits through non-conventional time reversal. *J. Phys. A*, 35:1381, 2002.

[176] P. A. Braun et al. Statistics of self-crossings and avoided crossings of periodic orbits in the hadamard-gutzwiller model. *Eur. Phys.J. B*, 30:189, 2002.

[177] D. Spehner. Spectral form factor of hyperbolic systems: leading off-diagonal approximation. *J. Phys. A*, 36:7269, 2003.

[178] M. Turek and K. Richter. Leading off-diagonal contribution to the spectral form factor of chaotic quantum systems. *J. Phys. A*, 36:L455, 2003.

[179] S. Müller. Classical basis for quantum spectral fluctuations in hyperbolic systems. *Eur. Phys. J. B*, 34:305, 2003.

[180] S. Heusler et al. Universal spectral form factor for chaotic dynamics. Preprint nlin.CD/0309022, 2003.

[181] E. J. Heller. Bound-state eigenfunctions of classically chaotic Hamiltonian systems – scars of periodic orbits. *Phys. Rev. Lett.*, 53:1515, 1984.

[182] E. B. Bogomolny. Smoothed wave-functions of chaotic quantum-systems. *Physica D*, 31:169, 1988.

[183] M. V. Berry. Quantum scars of classical closed orbits in phase-space. *Proc. R. Soc. London Ser. A-Math. Phys. Eng. Sci.*, 423:219, 1989.

[184] S. Tomsovic and E. J. Heller. Semiclassical construction of chaotic eigenstates. *Phys. Rev. Lett.*, 70:1405, 1993.

[185] O. Agam and S. Fishman. Semiclassical criterion for scars in wave-functions of chaotic systems. *Phys. Rev. Lett.*, 73:806, 1994.

[186] S. Fishman, B. Georgeot, and R. E. Prange. Fredholm method for scars. *J. Phys. A*, 29:919, 1996.

[187] S. Fishman. Wave functions, Wigner functions and Green functions of chaotic systems. In I. V. Lerner, J. P. Keating, and D. E. Khmelnitskii, editors, *Proceedings of a NATO Advanced Study Institute on Supersymmetry and Trace Formulae: Chaos and Disorder*, volume B370 of *the NATO ASI Series*, page 193. Kluwer Academic/Plenum, New York, 1998.

[188] L. Kaplan and E. J. Heller. Linear and nonlinear theory of eigenfunction scars. *Ann. Phys.*, 264:171, 1998.

[189] F. Faure, S. Nonnenmacher, and S. D. Bievre. Scarred eigenstates for quantum cat maps of minimal periods. *Commun. Math. Phys.*, 239:449, 2003.

[190] P. B. Wilkinson et al. Observation of 'scarred' wavefunctions in a quantum well with chaotic electron dynamics. *Nature*, 380:608, 1996.

[191] J. P. Bird, R. Akis, and D. K. Ferry. Experimental signatures of wave-function scarring in open semiconductor billiards. *Phys. Scr.*, T90:50, 2001.

[192] A. Kudrolli, M. C. Abraham, and J. P. Gollub. Scarred patterns in surface waves. *Phys. Rev. E*, 6302:026208, 2001.

[193] C. Gmachl et al. Kolmogorov-Arnold-Moser transition and laser action on scar modes in semiconductor diode lasers with deformed resonators. *Opt. Lett.*, 27:824, 2002.

[194] T. Harayama et al. Lasing on scar modes in fully chaotic microcavities. *Phys. Rev. E*, 67:015207, 2003.

[195] R. L. Waterland et al. Classical-quantum correspondence in the presence of global chaos. *Phys. Rev. Lett.*, 61:2733, 1988.

[196] D. Wintgen and A. Honig. Irregular wave-functions of a hydrogen-atom in a uniform magnetic field. *Phys. Rev. Lett.*, 63:1467, 1989.

[197] B. Eckhardt, G. Hose, and E. Pollak. Quantum-mechanics of a classically chaotic system - observations on scars, periodic orbits, and vibrational adiabaticity. *Phys. Rev. A*, 39:3776, 1989.

[198] B. W. Li. Numerical study of scars in a chaotic billiard. *Phys. Rev. E*, 55:5376, 1997.

[199] A. I. Shnirelman. *Usp. Mat. Nauk*, 29:181, 1974.

[200] S. W. McDonald and A. N. Kaufman. Wave chaos in the stadium - statistical properties of short-wave solutions of the Helmholtz-equation. *Phys. Rev. A*, 37:3067, 1988.

[201] B. W. Li and M. Robnik. Statistical properties of high-lying chaotic eigenstates. *J. Phys. A*, 27:5509, 1994.

[202] S. Fishman et al. Approach to ergodicity in quantum wave functions. *Phys. Rev. E*, 52:5893, 1995.

[203] K. Müller et al. Statistics of wave functions in disordered and in classically chaotic systems. *Phys. Rev. Lett.*, 78:215, 1997.

[204] L. Kaplan and E. J. Heller. Weak quantum ergodicity. *Physica D*, 121:1, 1998.

[205] A. Bäcker, R. Schubert, and P. Stifter. Rate of quantum ergodicity in Euclidean billiards. *Phys. Rev. E*, 57:5425, 1998.

[206] J. Stein and H. J. Stöckmann. Experimental-determination of billiard wave-functions. *Phys. Rev. Lett.*, 68:2867, 1992.

[207] D. Weiss et al. Quantized periodic orbits in large antidot arrays. *Phys. Rev. Lett.*, 70:4118, 1993.

[208] R. Fleischmann, T. Geisel, and R. Ketzmerick. Quenched and negative Hall-effect in periodic media - application to antidot superlattices. *Europhys. Lett.*, 25:219, 1994.

[209] H. Linke et al. Experimental tunneling ratchets. *Science*, 286:2314, 1999.

[210] H. Linke et al. Chaos in quantum ratchets. *Phys. Scr.*, T90:54, 2001.

[211] H. Schanz, R. Ketzmerick, and T. Dittrich, 2004. In preparation.

[212] S. Flach, O. Yevtushenko, and Y. Zolotaryuk. Directed current due to broken time-space symmetry. *Phys. Rev. Lett.*, 84:2358, 2000.

[213] P. Reimann. Brownian motors: noisy transport far from equilibrium. *Phys. Rep.*, 361:57, 2002.

[214] R. D. Astumian and P. Hänggi. Brownian motors. *Phys. TODAY*, 55:33, 2002.

[215] R. P. Feynman, R. B. Leighton, and M. Sands. *The Feynman Lectures on Physics.* Addison-Wesley, Reading, MA, 1966.

[216] F. Jülicher, A. Ajdari, and J. Prost. Modeling molecular motors. *Rev. Mod. Phys.*, 69:1269, 1997.

[217] A. van Oudenaarden and S. G. Boxer. Brownian ratchets: Molecular separations in lipid bilayers supported on patterned arrays. *Science*, 285:1046, 1999.

[218] L. R. Huang et al. Role of molecular size in ratchet fractionation. *Phys. Rev. Lett.*, 89, 2002.

[219] S. Matthias and F. Müller. Asymmetric pores in a silicon membrane acting as massively parallel brownian ratchets. *Nature*, 424:53, 2003.

[220] P. Jung, J. G. Kissner, and P. Hänggi. Regular and chaotic transport in asymmetric periodic potentials: Inertia ratchets. *Phys. Rev. Lett.*, 76:3436, 1996.

[221] J. L. Mateos. Chaotic transport and current reversal in deterministic ratchets. *Phys. Rev. Lett.*, 84:258, 2000.

[222] T. Dittrich et al. Classical and quantum transport in deterministic Hamiltonian ratchets. *Ann. Phys.-Berlin*, 9:755, 2000.

[223] V. I. Arnold. *Sov. Mat. Dol.*, 5:581, 1964.

[224] T. S. Monteiro et al. Proposal for a chaotic ratchet using cold atoms in optical lattices. *Phys. Rev. Lett.*, 89:194102, 2002.

Appendix A

Selected Publications

A01: Spectral statistics in chaotic systems
with two identical connected cells
T. Dittrich, B. Mehlig, H. Schanz and G. Koboldt
J. Phys. A 32 (1999) 6791-6820.

A02: Spectral statistics for quantum graphs:
Periodic Orbits and Combinatorics
H. Schanz and U. Smilansky
Phil. Mag. B 80 (2000) 1999-2021.

A03: Periodic-orbit theory of Anderson localization on graphs
H. Schanz and U. Smilansky
Phys. Rev. Lett. 84 (2000) 1427-1430.

A04: The leading off-diagonal correction
to the form factor of large graphs
G. Berkolaiko, H. Schanz and R. S. Whitney
Phys. Rev. Lett. 88 (2002) 104101.

A05: Form factor for a family of quantum graphs:
An expansion to third order
G. Berkolaiko, H. Schanz and R. S. Whitney
J. Phys. A: 36 (2003) 8373.

A06: Shot noise in chaotic cavities from action correlations
H. Schanz, M. Puhlmann and T. Geisel
Phys. Rev. Lett., 91 (2003) 134101.

A07: Scars on quantum networks ignore
the Lyapunov exponent
H. Schanz and T. Kottos
Phys. Rev. Lett. 90 (2003) 234101.

A08: Signature of chaotic diffusion in band spectra
T. Dittrich, B. Mehlig, H. Schanz and U. Smilansky
Phys. Rev. E 57 (1998) 359-365.

A09: Spectral correlations in systems undergoing
a transition from periodicity to disorder
T. Dittrich, B. Mehlig, H. Schanz, U. Smilansky,
P. Pollner and G. Vattay
Phys. Rev. E 59 (1999) 6541-6551

A10: Classical and quantum Hamiltonian ratchets
H. Schanz, M.-F. Otto, R. Ketzmerick and T. Dittrich
Phys. Rev. Lett. 87 (2001) 070601.

A11: Eigenstates ignoring regular and chaotic
phase-space structures
L. Hufnagel, R. Ketzmerick, M.-F. Otto and H. Schanz
Phys. Rev. Lett. 89 (2002) 154101.